

**Author**

Aaron P. R. Eberle,<sup>\*,†</sup> Donald G. Baird,<sup>†</sup> Peter Wapperom<sup>‡</sup>

**Address**

<sup>†</sup>Department of Chemical Engineering, Virginia Tech, 133 Randolph Hall, Blacksburg, Virginia, 24061, and <sup>‡</sup>Department of Mathematics, Virginia Tech, 572 McBryde Hall, Blacksburg, Virginia, 24061

**Correspondence**

To whom correspondence should be addressed. Tel.: (540) 231-7870. Fax: (540) 231-5022. E-mail: eberle@vt.edu

**Title**

The rheological properties of non-Newtonian fluids containing glass fibers: A review of experimental literature

**Abstract**

The objective of this review is to elucidate the rheological behavior of glass fiber suspensions whose suspending mediums are non-Newtonian fluids. In particular, this review focuses on determining the impact of fiber concentration, aspect ratio, orientation distribution, interaction with the suspending medium and suspending medium viscoelasticity on the rheology of glass fiber composite fluids. The presence of glass fiber can induce a yield-like behavior causing shear thinning to occur at reduced shear rates. Glass fiber can impede the elastic properties of the suspending medium but enhance the first normal stress function. Large stress overshoots in both the shear and normal stress growth functions are observed which are associated with changes in fiber orientation. Upon cessation of flow, stress relaxation follows that of the suspending medium but fibers retain their orientation. The presence of glass fiber can induce extension rate thinning and suppress the strain thickening behavior of the suspending medium.

**Key words**

Key words: glass fiber, suspension, nonlinear, rheology, composite, non-Newtonian

**1. Introduction**

Glass fibers have been used for decades to improve the mechanical, thermal and isolative properties of polymers.<sup>1</sup> These property improvements are highly dependent on the orientation distribution of the glass fiber. This makes it desirable to not only be able to predict the rheological behavior of the composite fluid but the orientation of the fiber, within the fluid or melt, generated during processing. Understanding the rheological behavior of polymeric fluids containing glass fibers is essential to model development. With respect to the fiber, it is of interest to understand the role of concentration and aspect ratio and their relation to the degree of inter-particle interaction (fiber-fiber) as well as orientation distribution and interaction with the suspending medium. With respect to the suspending medium it is of interest to understand the role of viscoelasticity and how it is affected by the presence of the fibers. The rheological properties of glass

fiber suspensions in Newtonian suspending mediums has been reviewed in detail by Ganani and Powell<sup>2</sup> and Zirnsak et al.<sup>3</sup> and will be referred to in this review for comparison purposes only. The primary focus of this review is to elucidate the rheological properties of glass fiber suspensions in non-Newtonian fluids of various degrees of viscoelasticity with an emphasis on composite fluids.

Before reviewing the rheology it is imperative to have a basic understanding of how glass fiber suspensions are prepared and how the fibers interact with the suspending medium. For this reason, subsequently, we will briefly discuss the methods used to compound or incorporate glass fibers into fluids and the use of surface treatments to increase the interaction with the matrix. We then classify fiber suspensions by their concentration and length. This is followed by a review of the different rheometers and rheometer geometries used to characterize glass fiber suspensions including a discussion of their strengths and weaknesses with respect to obtaining accurate measurements of rheological material functions. Lastly, we discuss and estimate the contribution of Brownian motion and gravity (relating to particle sedimentation) to changes in fiber orientation within the suspension.

**1.1. Suspension Preparation.** The four basic approaches to incorporating glass fiber into a non-Newtonian fluid are direct melt compounding, pultrusion, batch mixing, and in-situ polymerization.<sup>4</sup> Direct melt compounding is the most common industrial and economical method, generally accomplished with an extruder. The high degree of shear stress within the extruder results in a well dispersed composite but can severely degrade the overall fiber length and increase the fiber polydispersity.<sup>5</sup> Pultrusion is similar to the technique used in wire coating, in which a bundle of parallel continuous fibers are forced through a heated die and encapsulated by a polymer sheath. The continuous strand can then be cut or pelletized to the desired length. Pultrusion yields composites in a pellet form with a narrow fiber length distribution, but the fibers are generally concentrated at the center of the pellet resulting in imperfect wetting and dispersion of the fibers by the polymer.<sup>4</sup> Pultrusion can yield large weight percent, long fiber composite pellets that can then be processed with some form of an extruder where fiber length degradation is a repeat issue. Batch mixing is typically used to create small amounts of a specific suspension with minimal degradation to the overall fiber length. In-situ polymerization can yield composites of varying orientation from isotropic to collimated, where the fibers are completely wetted by the matrix material.<sup>4</sup> Like batch mixing, this method is typically not economically feasible for large scale production. Currently in-situ polymerization is used in industry to apply functional coatings or surface treatments. Experiments using ideal suspensions (i.e. suspensions with a uniform fiber length) formed by pultrusion, batch mixing and in-situ polymerization can help delineate the contribution of fiber length from concentration on the rheological properties.

**1.2. Surface Modifications.** The surface of a glass fiber is typically modified for two reasons: to minimize the self-destructive abrasive contact between the fibers and to increase the fiber-matrix interaction of the melt and adhesive strength of the composite. The use of “sizing” as a surface treatment has become an industrial standard and addresses both the abrasive contact and surface interaction. Sizing is a functional coating that acts as an abrasive barrier that is tailored to transfer stress from the matrix to the fiber reinforcement.<sup>6</sup> Though manufacturers are reticent about revealing the complete chemical formulation, typically sizing consists of a water-based mixture containing a

lubricant, film forming agent and a coupling agent that is applied in the form of a solution or aqueous emulsion. This creates a polymeric film on the fiber surface, of which, epoxy and poly(vinyl acetate) are common forms.<sup>7</sup> Coupling agents increase surface interaction and promote adhesion between the fiber and the polymeric matrix.<sup>8</sup> This is typically accomplished by molecules containing a silane group with an aliphatic branch or tail such as methacryloxypropyltrimethoxysilane (MPS) or phenyltriethoxysilane (PTS).<sup>9, 10</sup> The silane group is hydrolyzed at the glass surface to form silanols which form hydrogen bonds with the hydroxyl groups on the glass surface. Upon drying, a condensation polymerization occurs to form a polysiloxane ring on the glass fiber surface.<sup>11</sup> With the siloxane section of the molecule preferentially bonded to the inorganic glass surface a favorable and robust interaction between the aliphatic section and the polymer matrix is accomplished.

Plasma polymerization can be used to further improve the surface adhesion between the matrix and the fiber surface.<sup>6</sup> In this process Ar, H<sub>2</sub>, O<sub>2</sub>, CO<sub>2</sub>, NH<sub>3</sub> or air plasma at the fiber surface is used to initiate chemical and physical reactions altering surface properties and morphology. This generates a more favorable surface for the coupling agent to bond.<sup>12</sup>

**1.3. Classifying Glass Fiber Suspensions by Concentration.** As discussed later, the dynamic behavior of fiber suspensions is highly dependent on the concentration and length of the fibers within the suspension. For this reason we define three concentration régimes based on the degree of particle interaction and fiber excluded volume, as *dilute*, *semi-dilute*, and *concentrated*. Following the theory of Doi and Edwards, we consider a suspension of  $n$  fibers per unit volume, of equal length  $L$ , diameter  $d$  and corresponding aspect ratio  $a_r = L/d$ . The fiber concentration described through the volume fraction  $\phi$  is defined as

$$\phi = \frac{\pi n L d^2}{4} = \frac{\pi n L^3}{4 a_r^2} \quad (1)$$

For comparison purposes, subsequently we will report the volume fraction limits associated with the three concentration régimes for a test fiber of  $d = 15 \mu\text{m}$  and  $L = 1.5 \text{ mm}$  with corresponding  $a_r = 100$ .

**(a) Dilute Régime.** The *dilute* régime is described as one having a sufficiently low concentration of fibers in which a fiber is free to rotate without interference from contact with other fibers. Furthermore, it is assumed there is no hydrodynamic interaction. Theoretically, this occurs when the average distance between the center of mass of two rods is greater than  $L$ . Therefore, a perfectly disperse suspension must obey the constrain  $n < 1/L^3$  to be considered *dilute*. This can be related to the fiber aspect ratio and volume fraction by  $4\phi < \pi a_r^{-2}$  which is roughly  $\phi < a_r^{-2}$ . A *dilute* suspension containing our test fiber would be subject to the constraint  $\phi < 0.0001$ .

**(b) Semi-dilute Régime.** The *semi-dilute* régime is such that hydrodynamic interaction, as a result of the relatively close proximity between fibers, is the predominant phenomena and some physical contact between fibers is present. However, the suspension orientation state is not subject to geometric constraints, i.e. can be completely random. Doi and Edwards describe a *semi-dilute* suspension of rod-like molecules as one whose dynamic properties are affected but the static properties are not.<sup>13</sup> Interaction

between fibers is achieved when  $n > 1/L^3$  but when the mean spacing between fibers,  $S_m$ , is on the order of the diameter of the fiber, physical contact between rods becomes an increasingly significant phenomena; therefore the upper limit is subject to the constraint  $S_m \gg d$ .<sup>14</sup> The mean spacing between fibers is a function of the orientation state of the rods within the suspension. For a random orientation state the mean spacing is estimated as  $S_m \cong 1/(nL^2)$  and for a suspension whose fibers are completely aligned the mean spacing is of the order  $S_m \cong (nL)^{-1/2}$ .<sup>15, 16</sup> This leads to two upper limits:  $n \ll 1/(dL^2)$  for random and  $n \ll 1/(d^2L)$  for aligned orientation. This can be related to the fiber aspect ratio and volume fraction by  $\phi \ll (\pi/4)a_r^{-1}$  which is roughly  $\phi \ll a_r^{-1}$  and  $\phi \ll \pi/4$  respectively. A randomly oriented, *semi-dilute* suspension containing our test fiber would be subject to the constraints  $0.0001 < \phi < 0.01$ .

**(c) Concentrated Régime.** The *concentrated* régime is where  $n \geq 1/(dL^2)$  or  $\phi \geq a_r^{-1}$ . In this range the dynamic properties of the rods can be severely affected by fiber-fiber interactions and can lead to solid-like behavior.<sup>14</sup> Above some critical concentration  $\phi^*$ , rod-like molecules will preferentially align and become nematic. Doi and Edwards estimated the critical concentration to be  $\phi^* \cong 4a_r^{-1}$  and Flory<sup>17</sup> estimated  $\phi^* \cong 12.5a_r^{-1}$ . It is not clear whether fibers within a suspension will also preferentially align but it seems reasonable, for rigid fibers, that geometric constraints would cause this to occur. A *concentrated* suspension containing our test fiber would be subject to the constraint  $\phi > 0.01$  and the critical concentration for alignment, following Doi and Edwards, would be  $\phi^* \cong 0.04$ . As a note, glass fiber composites of industrial interest typically have fiber concentrations of  $\phi > 0.1$ .

**1.4. Classifying Glass Fiber Suspensions by Length.** In suspensions containing a distribution of fiber lengths the two most common averaging techniques used are the number average ( $L_n$ ) and weight average ( $L_w$ ) defined as

$$L_n = \frac{\sum_i n_i L_i}{\sum_i n_i} \quad (2)$$

$$L_w = \frac{\sum_i n_i L_i^2}{\sum_i n_i L_i} \quad (3)$$

The majority of the literature refers to the number average when calculating  $a_r$  and in defining the concentration régime of interest and will be used for this review unless otherwise specified.

Huq and Azaiez<sup>18</sup> compared the steady shear viscosity of mono-disperse and poly-disperse suspensions and found that of the standard fiber length averages  $L_w$  gave the best representation, but was still inaccurate at representing the effect of fiber length on the shear viscosity. Their study suggested that the following average, termed here as  $L_{HA-avg}$ , was more appropriate and is defined as

$$L_{HA-avg}^2 = \frac{\sum_i n_i L_i^3}{\sum_i n_i L_i} \quad (4)$$

The authors state that this average is only valid for the *dilute* and *semi-dilute* concentration régime.

In general, the fiber length of glass fiber suspensions is divided into two classes: short and long. Exactly what determines a fiber to be categorized as short or long is somewhat ambiguous, but usually short glass fiber suspensions contain fibers that are assumed to remain rigid during flow. Conversely, long glass fibers are ones that flex while the fluid is deformed. Kumar et al.<sup>19</sup> state that short glass fiber composites contain glass fibers with  $a_r < 100$ . Little work has been done to mathematically establish boundaries that separate short from long glass fiber suspensions. However, Forgacs and Mason<sup>20</sup> developed an equation to estimate the critical extra stress,  $\tau_{critical}$ , at which the shear-induced axial compression can cause a rotating fiber to buckle:

$$\tau_{critical} \cong \frac{E_f (\ln 2a_r - 1.75)}{2a_r^4} \quad (5)$$

where  $E_f$  is the flexural or bending modulus of the fiber. The authors found the equation to be in reasonably good agreement with experimental results for nylon, dacron and rayon fibers with diameters of 12.2, 7.8 and 3.5  $\mu\text{m}$  respectively, and various lengths resulting in aspect ratios ranging from 170-310. As an estimate this same approach can be applied to glass fibers. For glass fibers with  $a_r = 20, 60, 100$  and 600 the critical shear stress, using Eq. (5), is calculated to be  $\tau_{critical} = 4.4 \cdot 10^5, 8.5 \cdot 10^3, 1.3 \cdot 10^3$  and 1.5 (Pa) respectively, assuming  $E_f \approx 73 \text{ GPa}$ .<sup>21</sup> Defining a fiber as short or long depends on the shear stress seen by the fiber within the fluid. In low shear stress flow fields (i.e. low shear rate rheometrical flows) fibers with  $a_r < \sim 100$  typically can be classified as short fibers. In high shear stress flow fields (i.e. injection molding) fibers with  $a_r < \sim 40$  typically can be classified as short fibers.

**1.5. Rheometry: Flow Field and Boundary Effects.** Many different shear rheometers have been used to characterize the rheology of fiber suspensions. The most commonly used for polymer melt suspensions are torsional and capillary rheometers and, in a few instances, sliding plate rheometers.<sup>22</sup> Also, for low viscosity suspensions concentric cylinder<sup>18, 23</sup>, falling ball<sup>24</sup>, and Couette<sup>25</sup> viscometers have been used. It is of importance to note that the type of rheometer used to characterize a fluid containing relatively large particles when compared to the rheometer flow field dimensions may influence the rheology. This can occur through boundary interactions, flow field complications associated with curvilinear streamlines and particle migration during testing. Subsequently, we review the strengths and weaknesses of the different rheometers used to characterize glass fiber suspensions. First, we look at torsional and sliding plate shear rheometers followed by pressure driven flow capillary rheometers.

**(a) Torsional Rheometers.** Torsional rheometers are commonly used to characterize the low shear rate rheology of glass fiber suspensions. Traditionally, this type of rheometer utilizes cone-and-plate (CPR) or parallel-plate (PPR) fixtures with

small gaps (CPR  $\sim$  .05 mm, PPR  $\sim$  0.5-2 mm) and plate diameters ranging from 25 – 75 mm. In general CPRs provide a homogeneous shear field but allow for no gap control and can impart a flow history on the sample as it is *squeezed* to proper gap dimensions. PPRs allow a certain amount of gap control but the shear rate varies from the center of the plate to the outer edge resulting in an inhomogeneous shear field. Because the rate of fiber rotation is dependent on the shear rate, an inhomogeneous shear field could result in increased fiber-fiber interaction during transient changes in the fiber microstructure. Exactly how this effects the rheology is unclear.

Boundary interactions can occur when the rheometer gap is small compared to the characteristic length of the filler.<sup>26</sup> For a fiber, the characteristic length can significantly change depending on its orientation. For instance, a fiber whose orientation is in the shear direction has a characteristic length that is equal to the length of the fiber, while a fiber that is aligned in the flow direction has a characteristic length equal to the diameter of the fiber.<sup>26</sup> Glass fibers in composite fluids of industrial interest typically have a diameter on the order of 10  $\mu$ m with the majority between 13-16  $\mu$ m and average lengths which range from roughly 0.1-12.5 mm and in some cases exceed 25 mm. To minimize fiber-boundary interaction Blankeney<sup>23</sup>, and Attanasio et.al.<sup>27</sup> suggested that the sample thickness should be greater than three times the characteristic length of the filler. Mondy et al.<sup>28</sup> calculated that for a non-spherical particle to maintain its periodic rotation - mathematically described by Jeffery<sup>29</sup> and termed “Jeffery orbit”- the distance between the boundaries must be greater than four times the characteristic length of the particle.

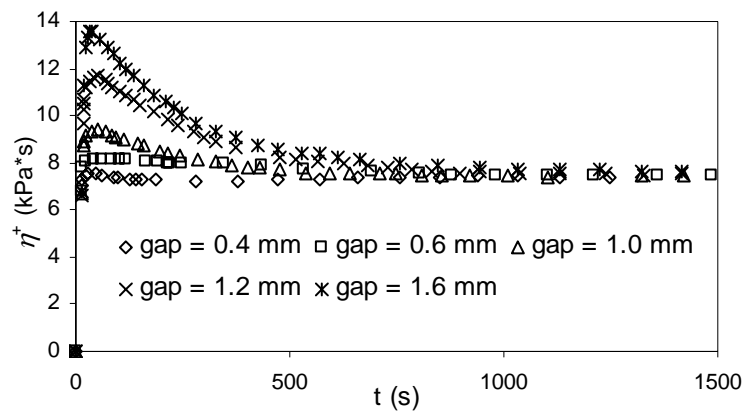


**Figure 1.** Effect of gap height, in a torsional PPR, on the shear stress growth coefficient in start-up of shear flow for a glass fiber-filled polypropylene (PP),  $\phi = 0.0354$ , the fiber length was not given.<sup>30</sup>

Boundary interactions are most probable in the case of a fiber tumbling in the shear plane. Fig. 1 is a plot of the shear stress growth coefficient in start-up of shear flow for a glass fiber-filled polypropylene (PP) with increasing gap in a PPR; the length of the fiber was not given.<sup>30</sup> The shear stress growth coefficient is clearly dependent on the gap height in the initial start-up region; the magnitude of the overshoot is greater for experiments performed with a larger rheometer gap. However, the steady-state value is unaffected by gap height. This is believed to be a result of the boundaries interfering with fiber end-over-end rotation during start-up of shear flow for a sample whose initial

fiber orientation is not aligned in the flow direction. Sepehr et al.<sup>31</sup> found minimal gap height dependence above a gap height of 1.4 mm in a PPR for a suspension containing glass fibers with an average length of 0.26 mm.

In the case of torsional shear devices the presence of curvilinear streamlines may also lead to problems in rheological measurements of glass fiber suspensions. The problems occur when the fibers try to establish an orientation of least resistance to flow, which is aligned parallel with the streamlines. Rigid fibers can never fully align themselves in the curvilinear streamlines. Although there is no recorded quantification of this factor it must be taken into consideration in the accuracy of the rheological measurements in torsional devices, especially in the case of long fibers.

**(b) Sliding Plate Rheometers.** In an attempt to reduce the error associated with torsional rheometers Owen et al.,<sup>32</sup> Laun,<sup>33</sup> and Ericsson et al.<sup>22</sup> employed a sliding plate rheometer that generates a rectilinear flow field. No indication was given on the ability to perform transient experiments where fiber tumbling and boundary interaction could be an issue. However, theoretically, very large gaps can be employed which could reduce error associated with fiber-boundary interactions. As a note, no estimations were made about error reduction associated with this flow geometry compared to torsional rheometers but it is believed that this type of rheometer represents an improvement in obtaining accurate measurements of rheological behavior.<sup>22</sup> The limitation in using a sliding plate rheometer is the maximum strain that one can achieve, which is dependent on rheometer design and gap height.

**(c) Capillary Rheometers.** Capillary rheometers have traditionally been used to investigate the deformation behavior of fiber suspensions at high shear rates. In this case the suspension is forced through an abrupt contraction and the pressure drop is measured across the contraction and capillary length. Studies have shown that particle migration can occur away from the channel wall across streamlines, in laminar flow, due to small inertia and wall effects termed “*tubular pinch*”. Experimentally, this was first observed by Segré and Silberberg<sup>34,35</sup> for a dilute suspension of neutrally buoyant spheres in flow through a pipe. As a result of the particle migration the authors found a maximum concentration at a radial position from the centerline to pipe radius ratio ( $r/R$ ) of 0.6. Koh et al.<sup>36</sup> discovered similar results in which a concentration maximum was found near the center in a rectangular channel for a concentrated suspension using an experimental adaptation to the laser-Doppler anemometry technique. Conversely, Wu<sup>37</sup> reported the opposite behavior for a short glass fiber-filled polyethylene terephthalate (PET) where he found the concentration of fiber to deplete near the relative radial position  $r/R = 0.63$  and accumulate near the surface and axis. Becraft and Metzner<sup>38</sup> found no large scale fiber migration but did find local variations in concentration. It is unclear if particle migration occurs with suspensions containing fibers. However, if migration does occur away from the boundaries as with spherical particles, the regions of highest shear rates, close to the capillary wall, could contain a far less concentration of fibers which results in a stress response similar to the pure matrix.<sup>39</sup>

**(d) Summary of Rheometers.** The rheological response of a suspension can be influenced by the rheometer used to characterize it.<sup>22</sup> The influences are a result of boundary interactions, flow field complications associated with curvilinear streamlines and possibly particle migration. Fiber-boundary interactions are most prevalent in the case of a fiber tumbling in the shear plane, as can be found in the start-up of shear flow

experiments, when the rheometer gap height is roughly the same size or smaller than the characteristic length of the fiber.<sup>26</sup> In this case the transient stress response can be masked by the boundaries interfering with fiber rotation as depicted in Fig. 1. Flow field geometry complications can occur in torsional rheometers or in any case where the rheometer flow field streamlines are curvilinear and significantly differ from the geometry of the particle. Inhomogeneous shear, as in PPRs, could potential exaggerate the degree of fiber interaction, of which, the effects on the rheology are unclear. Particle migration can possibly occur in the case of abrupt contractions in pressure driven flow rheometers (as in capillary rheometers). This behavior can result in a stress response similar to the matrix, masking the presence of the fiber.<sup>37</sup>

The statements above outline possible sources of error associated with typical melt rheometers used to characterize the rheological behavior of fiber suspensions. However, these rheometers have been widely used by researchers to characterize the rheology of fiber suspensions due to their availability and temperature control capabilities useful for polymer melts. As a result it is difficult to quantitatively asses the rheological behavior of glass fiber suspensions, especially long glass fiber suspensions, but the published rheological measurements still allow for qualitative relations to be made. Ideally, any rheological measurement should be performed in a “sufficiently large” device so that the boundary and flow field effects are minimized.<sup>26</sup>

**1.6. Impact of Brownian Motion and Sedimentation.** Subsequently, we discuss Brownian motion and sedimentation with the intent of clarifying the contributing forces that can lead to either dynamic or static changes in fiber orientation and position.

**(a) Brownian Motion.** Brownian motion refers to the random movement of a sufficiently small particle suspended in a fluid. The movement of the particle is a result of a random number of impacts of various strength from random directions by molecules of the suspending fluid. Therefore, the effects of Brownian motion are only seen in systems where the particles are small enough to be affected by the bombardment of molecules. In a system of sufficiently small rods where Brownian motion effects are present (i.e. liquid crystalline molecules), the rods can be subject to two kinds of Brownian motion, translational and rotational. Translational Brownian motion is the random motion of a position vector indicating the center of mass of the rod and rotational Brownian motion is the random motion of the unit vector around the center of mass.<sup>13</sup>

The most common way to determine if a particle is affected by Brownian motion is to calculate the Péclet number (Pé). The Péclet number is defined as the dimensionless ratio of the shear rate,  $\dot{\gamma}$ , to the rotational diffusion constant,  $D_r$ . The rotational diffusion constant represents the rate at which a particle changes its orientation with respect to rotational Brownian motion.  $D_r$  is defined as

$$D_r = \frac{k_B T}{\xi_r} \quad (6)$$

where  $k_B$  is Boltzmann’s constant,  $T$  is the temperature in Kelvin and  $\xi_r$  is the rotational friction constant. For a cylinder of  $a_r > 3$  the rotational friction constant is given by

$$\xi_r = \frac{\pi\eta_s L^3}{3[\ln(a_r) - \alpha]} \quad (7)$$

where  $\eta_s$  is the viscosity of the suspending medium and  $\alpha$  is a correction factor. Calculations based on the point force approximation give  $\alpha = 0.8$  as a good estimate.<sup>40</sup> At small  $Pé$ , Brownian effects are significant and can dominate the rod motion leading to particle orientations, under static conditions, that are close to random. Conversely, at high  $Pé$  the effects of Brownian motion are insignificant and hydrodynamic forces dominate particle motion. For comparison purposes, a thermotropic copolyester liquid crystalline polymer commercial name Vectra A900 (copolyester of 27 mole % 2-hydroxy-6-naphthoic acid and 73 mole % hydroxybenzoic acid) has a  $D_r \sim 12.2 \text{ s}^{-1}$  at its melt temperature of 283°C, while a short glass fiber ( $L = 0.5 \text{ mm}$ ,  $d = 15 \text{ }\mu\text{m}$ ) in a suspending medium with  $\eta_s = 1,000 \text{ Pa}\cdot\text{s}$  at 200 C has a  $D_r \sim 10^{-13} \text{ s}^{-1}$ . Larson<sup>41</sup> makes the statement that a particle whose longest dimension exceeds  $\sim 10 \text{ }\mu\text{m}$  can be considered non-Brownian.

**(b) Sedimentation.** To support discussion later in the review it is of interest to estimate the effect that gravity has on a fiber within a fluid. Chaouche and Koch<sup>42</sup> proposed an expression to estimate the relative time scale for sedimentation  $t_s$ , the time required for a fiber parallel to the vertical direction to sediment over its length, as

$$t_s = \frac{8\eta_s L}{\Delta\rho g d^2 [\ln(2a_r) - 0.72]} \quad (9)$$

where  $\Delta\rho$  difference between the densities of the suspending medium and the particle and  $g$  is the acceleration due to gravity. The sedimentation time scale for our test fiber ( $d = 15 \text{ }\mu\text{m}$  and  $L = 1.5 \text{ mm}$ ,  $\rho = 2.617 \text{ g/cm}^3$ ) in a fluid of  $\eta_s = 100 \text{ Pa}\cdot\text{s}$  ( $\rho = 0.9 \text{ g/cm}^3$ ) using this approach is calculated to be  $t_s \sim 19 \text{ hr}$ . As a comparison, the sedimentation time scale for a similar suspension with  $\eta_s = 10 \text{ Pa}\cdot\text{s}$  and fiber  $L = 0.15 \text{ mm}$  is estimated to be  $t_s \sim 0.4 \text{ hr}$ . This time increases with fiber length and is proportional to the viscosity of the suspending medium. Obviously, this basic estimation does not take into account fiber-fiber interactions that would also act to increase the sedimentation time. In glass fiber suspensions of very small fibers in low viscosity fluids gravity could potentially effect fiber position and orientation. However, typically it is assumed that gravity has no effect on fibers in polymer melts.

## 2. Shear Rheology

**2.1. Steady Shear Flow.** In the case of simple shear flow, as found in rheometrical flows, the fluid velocity occurs in one direction only ( $v_1 = \dot{\gamma}x_2$ ,  $v_2 = v_3 = 0$ ) and the shear rate is assumed to be constant within the rheometer gap. With these assumptions and following the official nomenclature for material functions of viscoelastic fluids<sup>43</sup>, the non-Newtonian fluid shear viscosity  $\eta$ , can be defined through the shear stress as

$$\eta = \sigma / \dot{\gamma} \quad (10)$$

In the same manner, the first and second normal stress functions,  $N_1$  and  $N_2$  respectively, are defined as

$$N_1 = \sigma_{11} - \sigma_{22} \quad (11)$$

$$N_2 = \sigma_{22} - \sigma_{33} \quad (12)$$

In addition, we refer to  $N_1-N_2$  as the normal stress function difference. The subsequent review of literature pertaining to the shear rheology of glass fiber suspensions begins with the shear viscosity followed by a review of first and second normal stress functions.

**(a) Shear Viscosity.** The addition of glass fiber to either a Newtonian or non-Newtonian fluid enhances the shear viscosity when compared to the neat suspending medium, especially at low shear rates. The degree to which the shear viscosity is affected is a function of the fiber concentration, aspect ratio, and orientation distribution.<sup>26</sup> In the following review of the shear viscosity for glass fiber suspensions, the effect fiber concentration and aspect ratio have on Newtonian fluids is outlined first, as a basis for comparison to glass fiber suspensions in non-Newtonian fluids. We then review the effects of fiber concentration, aspect ratio, and shear history (i.e. orientation distribution) on shear viscosity of non-Newtonian fluids. Finally we consider the temperature dependence of the shear viscosity.

In general for suspensions of glass fibers in Newtonian fluids, in the *dilute* and *semi-dilute* fiber concentration régime, the shear viscosity has a linear dependence with fiber concentration, that increases with aspect ratio.<sup>44</sup> A deviation from this general trend was found by Milliken et al.<sup>24</sup> when they performed experiments on a suspension of short glass fibers ( $a_r = 19.8$ ) in a Newtonian suspending using a falling ball viscometer. Their results suggested that the shear viscosity dependence on the volume fraction of fibers changes from a linear correlation for *dilute* suspensions to a cubic dependence on volume fraction at the transition between *dilute* and *semi-dilute* concentrations. As a note, the aspect ratio was not varied in the experiment.

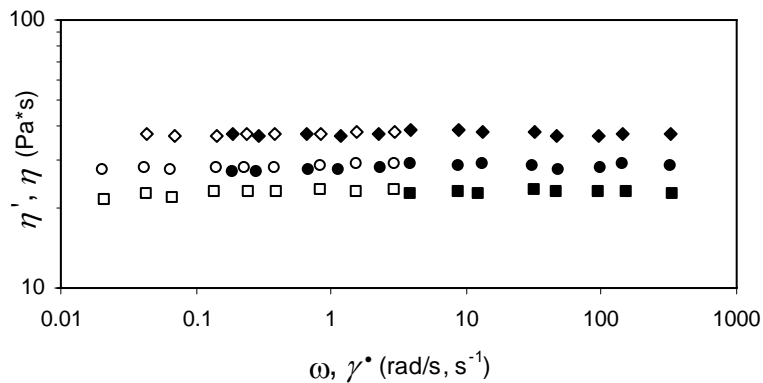


**Figure 2.** Shear viscosity vs. shear rate (filled symbols) and the dynamic viscosity vs. frequency (unfilled symbols) for short glass fibers ( $a_r = 24.3$ ) in a Newtonian suspending medium of various fiber concentration,  $\phi = 0$  ( $\blacksquare$ ,  $\square$ ),  $0.05$  *semi-dilute* ( $\bullet$ ,  $\circ$ ),  $0.08$  *concentrated* ( $\blacklozenge$ ,  $\lozenge$ ). All measurements were preformed on a torsional PPR.<sup>44</sup>

The presence of fiber has been shown to induce shear thinning characteristics in Newtonian fluids, the degree of which is dependent on the concentration and aspect ratio of the fiber. At low concentrations and small aspect ratios, in the *dilute* to *semi-dilute* concentration régimes, fiber suspensions in Newtonian suspending mediums show little to no dependence on shear rate, as shown in Fig. 2 (filled symbols). Fig. 2 is an example of the shear viscosity vs. shear rate for a Newtonian fluid containing various fiber concentrations of  $\phi = 0, 0.05$  (*semi-dilute*), and  $0.08$  (*concentrated*). The unfilled symbols represent the real component of the complex viscosity vs. frequency and will be commented on in section 2.2. (Small-Amplitude Oscillatory Shear Flow). In this case, the presence of glass fiber enhances the magnitude of shear viscosity, but it remains fairly constant over the complete range of shear rates tested. However, for suspensions containing higher concentrations, especially with large aspect ratio fibers the shear thinning behavior can be significant. Ganani and Powell<sup>44</sup> reviewed much of the literature in the area of glass fibers suspended in Newtonian fluids and found that for suspensions containing fibers with aspect ratios in the range of 35-45 a weak shear thinning behavior was noticed at low shear rates, followed by a Newtonian plateau at  $\dot{\gamma} > 10 \text{ s}^{-1}$ . For  $a_r > 100$ , the authors found a strong shear rate dependence that was seen over a shear rate range of  $0.1 - 100 \text{ s}^{-1}$ . The shear thinning behavior of non-*dilute* suspensions of glass fibers in a Newtonian fluid is explained by the destruction of transient network structures of fibers at increasing shear rates.<sup>3</sup>

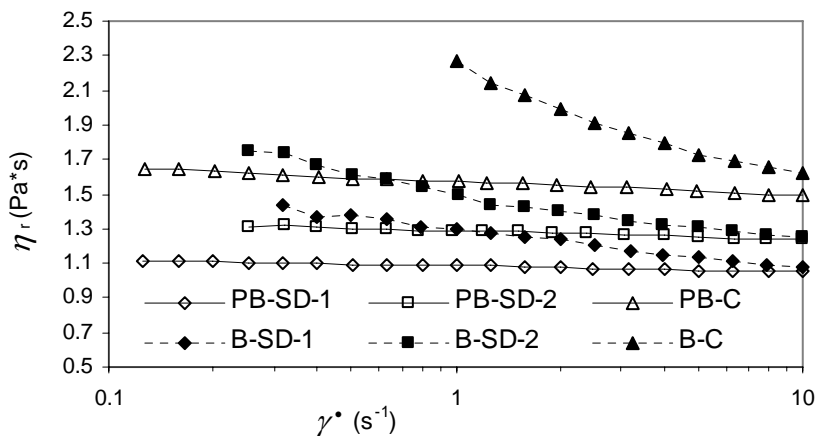
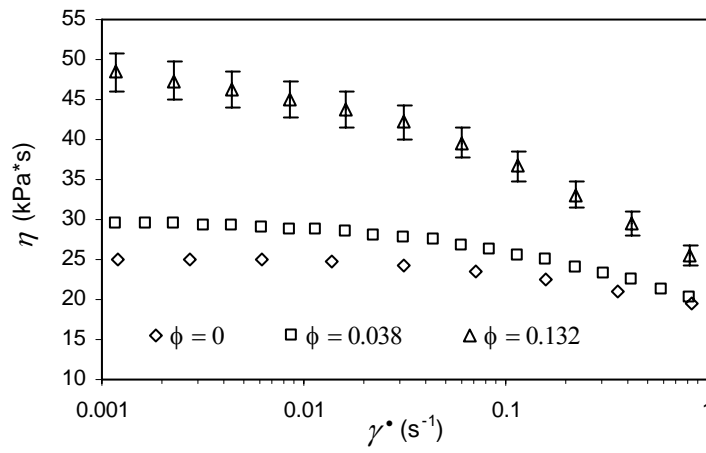


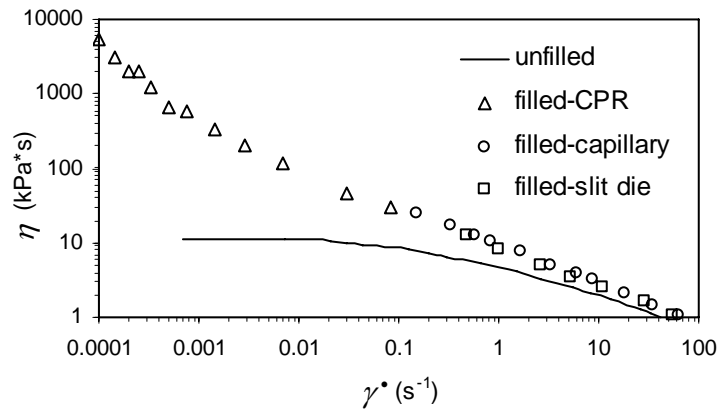
**Figure 3.** Reduced shear viscosity vs. shear rate for various concentrations of glass fiber ( $a_r \sim 20$ ) suspended in polybutene (PB, a Newtonian fluid) and a Boger fluid (B). The fiber volume fractions are  $\phi = 0.0158, 0.0327,$  and  $0.0706$  termed SD-1, SD-2 (*semi-dilute* régime) and C (*concentrated* régime) respectively. All measurements were performed on torsional PPR with gap-to-fiber length ratio greater than 3.<sup>31</sup>

The effect that the presence of glass fiber has on the shear viscosity significantly changes with the viscoelastic nature of the suspending medium. This behavior can be seen in Fig. 3 for two model suspensions containing short glass fibers of  $a_r \sim 20$ : a polybutene (PB) suspension (roughly a Newtonian fluid) and a Boger fluid suspension (a fluid that exhibits elastic behavior but has little shear rate dependence). Similar to the

suspensions in a purely Newtonian fluid, the reduced shear viscosity of the PB suspension increases in a linear manner with the fiber volume fraction. The reduced shear viscosity refers to the fiber suspension viscosity normalized by the viscosity of the suspending medium at constant temperature and pressure and shear rate,  $\eta_r \equiv \eta/\eta_s$ . Also, while it is difficult to detect, the authors state that the suspension exhibits a slight shear thinning behavior that was not present in the neat PB.<sup>31</sup> At similar fiber concentrations the fiber-filled Boger fluid exhibits an increasing yield-like behavior and greatly enhanced shear thinning characteristics. Interestingly, the Boger fluid is 91.0 mass % the same composition of the Newtonian fluid, with 0.6 mass % of a high MW polyisobutene, and 8.4 mass % kerosene. The polyisobutene is the source of the elastic properties and apparently lead to the enhanced effect of the fibers. It is thought that this behavior is a result of increased fiber-fiber interaction through a pseudo network formed by adsorption of the high molecular weight chains onto the glass fibers.<sup>31</sup> This interaction is increased and the effects enhanced by the use of surface treatments to the glass fiber.<sup>11, 39, 45</sup> However, due to the lack of published data, it is still unclear how fiber surface treatments exactly affect the rheology other than enhancing the interaction between the suspending medium and fibers.



(a)



(b)

**Figure 4.** Shear viscosity vs. shear rate. (a) Two short glass fiber-filled polypropylene

(PP) suspensions ( $\phi = 0.038$ ,  $a_r \sim 30$ , *semi-dilute* régime and  $\phi = 0.132$ ,  $a_r = 21.4$ , *concentrated* régime) and the neat suspending medium. The rheological experiments were performed on a PPR.<sup>46</sup> (b) Short glass fiber-filled high-density polyethylene HDPE ( $\phi = 0.136$ ,  $a_r = 30$ , *concentrated* régime) and the neat suspending medium.<sup>33</sup> The rheological experiments were performed with various rheometers as indicated in the figure legend.

The presence of glass fiber appears to have an even greater influence on the shear viscosity of suspensions whose suspending mediums are high molecular weight polymer melts, especially at low shear rates ( $\dot{\gamma} < \sim 10 \text{ s}^{-1}$ ).<sup>26, 31, 44, 47, 48</sup> This increases the difficulty in empirically delineating the dependence of the shear viscosity on the fiber concentration and aspect ratio. In general, the shear viscosity of suspensions containing a low concentration of low aspect ratio fiber (in the *dilute* and *semi-dilute* régime) usually approach a Newtonian plateau at low shear rates, and in many instances show little change from the behavior of the neat matrix.<sup>30</sup> The shear viscosity of suspensions containing a high concentration of fiber or fiber with a large aspect ratio (in the *concentrated* régime), exhibit a more pronounced behavior. At low shear rates the shear viscosity can exhibit a Newtonian plateau as shown in Fig. 4 (a) or rise in an unbounded manner and exhibit yield-like characteristics as shown in Fig. 4 (b). At high shear rates, shear thinning can occur at a reduced shear rate which can result in a shear viscosity similar to that of the neat suspending medium. Fig. 4 (a) shows the shear viscosity vs. shear rate for two short glass fiber-filled polypropylene (PP) suspensions at various concentrations and the neat suspending medium. The shear viscosity of the two suspensions ( $\phi = 0.038$ ,  $a_r \sim 30$ , *semi-dilute* régime and  $\phi = 0.132$ ,  $a_r = 21.4$  *concentrated* régime) appear to reach a Newtonian plateau at low shear rates, within the range of error. However, the increased fiber concentration causes the onset of shear thinning to occur at a lower shear rate. At high shear rates, the shear viscosity merges onto that of the neat matrix. Fig. 4 (b) shows the shear viscosity vs. shear rate of a short glass fiber-filled high-density polyethylene (HDPE) suspension ( $\phi = 0.136$ ,  $a_r = 30$ , *concentrated* régime) and the neat suspending medium.<sup>33</sup> In this case, the glass fiber suspension exhibits a yield-like behavior, and shows a shear thinning response over the whole shear rate range. This behavior is typical of a highly *concentrated* suspension of glass fibers in a non-Newtonian fluid, though deviations from this behavior do occur. Guo et al.<sup>1</sup> reported no yield-like behavior for a polymer suspension containing up to  $\phi = 0.384$  of short glass fiber in a linear low-density polyethylene with a melt flow index of 3.3. The authors do not discuss the use of surface treatments on the glass which could affect the interaction with the matrix nor give possible explanation of why no yield-like behavior was observed.

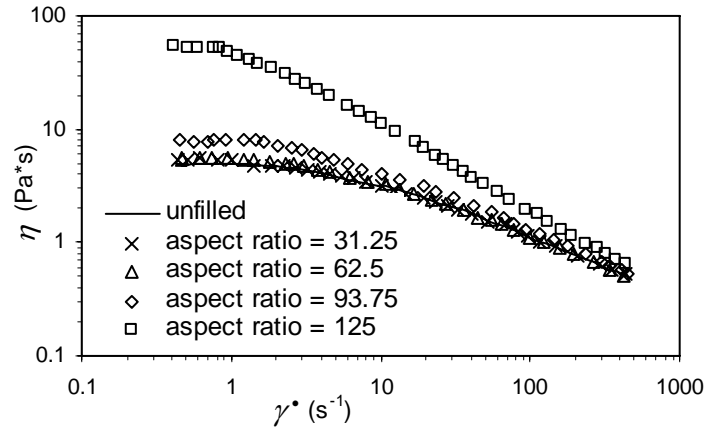


**Figure 5.** Shear viscosity vs. shear rate for glass fiber suspensions of various fiber length in a low viscosity non-Newtonian fluid with constant glass fiber concentration ( $\phi = 0.02$ ). The various suspensions have mono-disperse fiber lengths,  $L = 0.5, 1.0, 1.5,$  and  $2.0$  mm, and corresponding aspect ratios  $a_r = 31.25, 62.5, 93.75,$  and  $125$  respectively. The shortest glass fiber suspension related to the *semi-dilute* régime, the rest were *concentrated*. Rheological experiments were performed with a concentric cylinder rheometer.<sup>18</sup>

The shear viscosity is also highly dependent on fiber length which we describe through the aspect ratio. In general, higher aspect ratio fibers have a stronger contribution to the suspension shear viscosity, as seen in Fig. 5. Fig. 5 shows the shear viscosity vs. shear rate of a suspension of 3 wt% polyethylene oxide in water with  $\phi = 0.02$  of glass fiber of various mono-disperse aspect ratios. The suspension with the smallest aspect ratio relates to the *semi-dilute* concentration régime and the others are just above the *concentrated* régime boundary. The shear viscosity for the suspensions with the shortest aspect ratio show little deviation from the neat matrix, but the highest aspect ratio suspension shows a marked increase. Similar to other highly concentrated suspensions, whose shear viscosities deviate considerably from their neat counter parts, the suspension with the greatest aspect ratio exhibited shear thinning behavior at lower shear rates. Deviations from this general trend are scarce but can occur at very large fiber aspect ratios. Ericsson et al.<sup>22</sup> found little effect of fiber aspect ratio between values of  $a_r = 1050$  and  $2100$  for a suspension tested in a sliding plate rheometer. This was attributed to the inability of the long fiber to rotate out of plane and the fibers behaving more as continuous strands than as individual fibers.

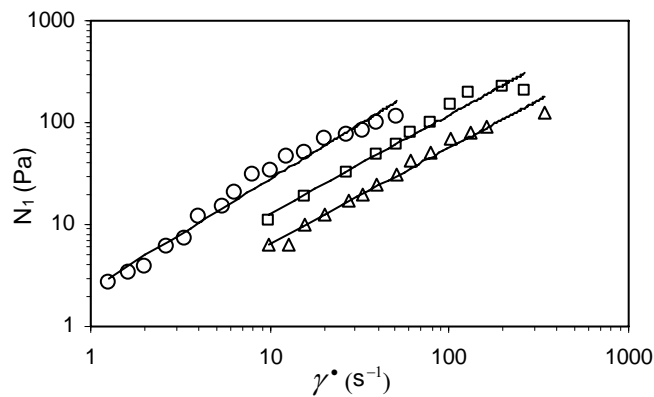
The more pronounced effect of fibers on shear viscosity at low shear rates and decreased effects at high shear rates is a reflection of changes in the suspension's microstructure.<sup>30</sup> It is speculated that changes in the fiber orientation distribution in a suspension during flow are irreversible and lead to shear history dependent rheology.<sup>30</sup> It is also speculated that a higher shear rate will impart a higher degree of fiber orientation in the flow direction.<sup>33</sup> As a result, a sample that is pre-sheared may not exhibit the same shear viscosity compared to a sample that has not been sheared or has an isotropic fiber orientation distribution.<sup>49</sup>

The presence of fiber has little to no influence on the temperature dependence of the shear viscosity.<sup>33, 46</sup> As with all liquids, the viscosity function of polymers and

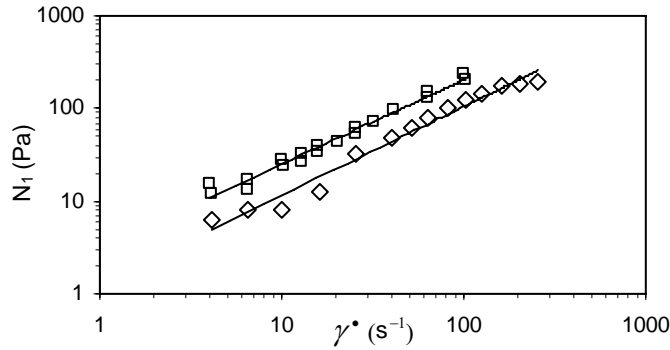
polymer suspensions decreases with increasing temperature.<sup>50</sup> However, the shape of the shear viscosity curve remains constant, even in the case of fiber suspensions where no zero shear viscosity is present.<sup>33</sup> Because of this, a master curve can be formulated using shift factors (time-temperature superposition) that for most polymeric fluids, follow an Arrhenius type temperature dependence.<sup>51</sup>

Though published information was limited, there was evidence by Greene and Wilkes<sup>52</sup> that glass fibers could reduce the molecular weight of the matrix material in an amount proportional to the concentration of fibers. The authors found this phenomenon to be evident in both polycarbonate and nylon materials, but had no influence on a polypropylene matrix. This behavior was attributed to mechanical degradation by the fibers, but no discussion was given to hydrolysis or thermal degradation as mechanisms for molecular weight reduction. The shift factors for fiber-filled non-Newtonian fluids are similar or the same as that of the neat suspending medium.

**(b) First and Second Normal Stress Function.** The first and second normal stress functions ( $N_1$  and  $N_2$ ) and the difference between them ( $N_1 - N_2$ ), defined by Eqs. (11) and (12), are typically limited to viscoelastic fluids. For unfilled Newtonian fluids both  $N_1$  and  $N_2$  are equal to zero. However, glass fiber suspensions with Newtonian suspending mediums can exhibit significant values of  $N_1$  and the presence of glass fiber can enhance  $N_1$  in viscoelastic fluids. The magnitude of the normal stress functions is dependent on the concentration and aspect ratio of the fiber and the elastic behavior of the matrix.<sup>26</sup> We first review the effect of fiber concentration and aspect ratio on the normal stress functions in Newtonian suspending mediums for comparison purposes. This is followed by a review of the effect that the glass fiber concentration and aspect ratio have on the normal stress functions in non-Newtonian suspending mediums.



(a)



(b)

**Figure 6.**  $N_1$  vs. shear rate. All measurements were performed on a torsional CPR. (a) Various glass fiber suspensions containing a constant fiber content ( $\phi = 0.044$ ,  $a_r = 276$ ) but different Newtonian suspending medium viscosities ( $\Delta$  14,  $\square$  16,  $\circ$  120 Pa\*s). (b) Two glass fiber suspensions of constant fiber concentration ( $\phi \sim 0.00046$ ) and Newtonian suspending medium with various fiber aspect ratio ( $a_r = \diamond$  276,  $\square$  552).<sup>3</sup>

Many workers have published non-zero values of  $N_1$  and  $N_1 - N_2$  for non-dilute glass fiber suspensions<sup>3, 31, 53, 54</sup> and other high aspect ratio filler suspensions<sup>55, 56</sup> with Newtonian suspending mediums.  $N_1$  is found to be dependent on the viscosity of the suspending medium, and the concentration and aspect ratio of the fiber. In general,  $N_1$  depends linearly on shear rate and by comparing  $N_1$  to  $N_1 - N_2$  it is typically found that  $N_2$  is negligible ( $-N_2 < 10\%$  of  $N_1$ ).<sup>3</sup> Fig. 6 (a) and (b) show  $N_1$  vs.  $\dot{\gamma}$  as a function of the viscosity of the Newtonian suspending medium and aspect ratio of the fiber, respectively; Fig. 7 (PB suspension) depicts the concentration dependence. In all three cases, increasing the suspending medium viscosity or the fiber aspect ratio and concentration increased the magnitude of  $N_1$  but the slope of  $N_1$  vs.  $\dot{\gamma}$  stayed roughly at unity.

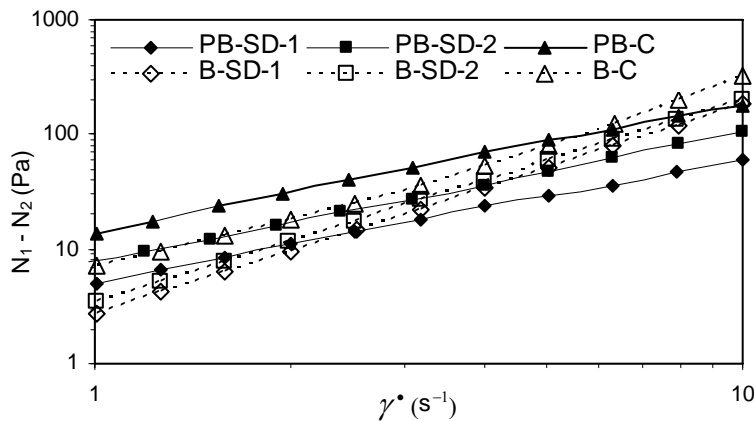


**Figure 7.**  $N_1 - N_2$  vs. shear rate for various concentrations of short glass fiber ( $a_r \sim 20$ ) suspended in polybutene (PB) and a Boger fluid (B). The fiber volume fractions are  $\phi = 0.0158$ ,  $0.0327$ , and  $0.0706$  termed SD-1, SD-2 (*semi-dilute régime*) and C (*concentrated régime*) respectively. All tests were performed on a torsional PPR with gap-to-fiber length ratio greater than 3.<sup>31</sup>

In general,  $N_I$  for fiber suspensions in non-Newtonian fluids follow a similar shear rate dependence as their unfilled counter part at some enhanced value, but in some cases can exhibit a plateau at low shear rates or merge onto the matrix value at high shear rates.<sup>30</sup> The enhanced values of  $N_I$  and  $N_I-N_2$  are believed to be the result of fiber-fiber interactions within the suspension.<sup>31</sup> In addition, fiber interaction can result in imperfect alignment of the fibers in the flow direction;<sup>57</sup> current theories for fiber suspensions in Newtonian fluids have shown that normal stresses arise when the fiber orientation has a component out of the plane of shear.<sup>58</sup> This behavior can be seen in Fig. 7 for a short glass fiber filled PB and Boger fluid. Fig. 7 is a graph of  $N_I-N_2$  vs.  $\dot{\gamma}$  for short glass fiber suspensions of constant  $a_r \sim 20$  with  $\phi = 0.05, 0.1$  and  $0.2$ . An interesting observation when comparing the PB (Newtonian-like) and Boger (viscoelastic) fluid suspensions is the PB suspension exhibits a more pronounced dependence of  $N_I-N_2$  on fiber concentration than the Boger fluid suspension. This behavior agrees with the work of Iso et al.<sup>47, 48</sup>, who compared the end-over-end fiber rotation of a dilute suspension of fibers suspended in a Newtonian and non-Newtonian fluid under simple shear flow conditions. Their experimental results suggest that the elastic nature of non-Newtonian fluids can compete with the fiber-fiber interactions. This same phenomenon is speculated to be the cause of higher values of  $N_I-N_2$  for the PB suspension at low shear rates compared to the values for the Boger fluid suspension.

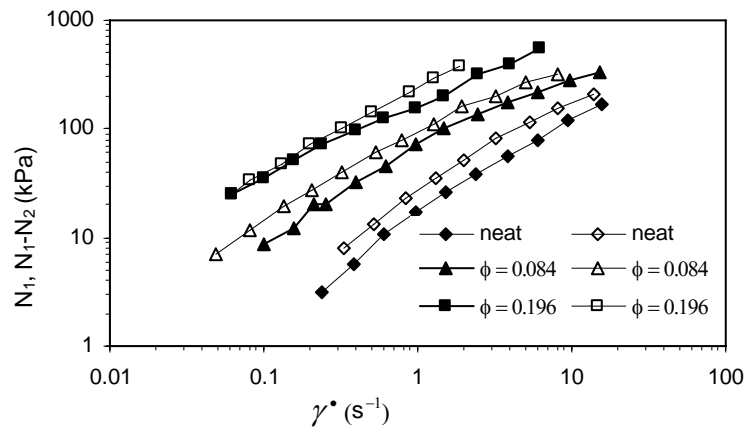


**Figure 8.**  $N_I$  and  $N_I-N_2$  vs. shear rate for a short glass fiber-filled HDPE ( $a_r = 157.5$  for  $\phi = 0.084$  and  $a_r = 78.7$  for  $\phi = 0.196$ ). The filled symbols represent  $N_I$  and the unfilled symbols  $N_I-N_2$ .  $N_I$  and  $N_I-N_2$  were obtained using a CPR and PPR, respectively.<sup>59</sup>

For highly elastic polymers  $N_2$  is not negligible but current literature suggests that it decreases with increasing fiber concentration. This behavior can be seen in Fig. 8 which is a graph of  $N_I$  and  $N_I-N_2$  vs. shear rate for two short glass fiber-filled HDPE suspensions of different fiber content. The presence of fiber enhances both  $N_I$  and  $N_I-N_2$  alluding to non-negligible values of  $N_2$ . However, at the highest concentration of fiber,  $\phi = 0.196$ ,  $N_I-N_2$  merges onto  $N_I$  which suggests the presence of fiber suppresses  $N_2$ .<sup>59</sup>

In general, the presence of glass fiber enhances  $N_I$  exhibited by non-Newtonian fluids. The most significant effect to the normal stresses is seen in the *concentrated* régime. The existence of non-negligible values of  $N_I$  in glass fiber suspensions in

Newtonian suspending mediums suggests that the enhanced normal stresses are a result of fiber interactions and not an enhancement to the elasticity of the suspending medium. Conversely, the presence of glass fiber seems to suppress the normal stresses resulting from the elasticity of suspending medium.

**2.2. Small-Amplitude Oscillatory Shear Flow.** We now consider the linear viscoelastic behavior of glass fiber-filled non-Newtonian fluids in small-amplitude oscillatory simple shear flow. These experiments involve the measurement of the unsteady response of a fluid when subject to sinusoidal deformations. The complex viscosity and complex modulus are defined as

$$\eta^*(\omega) = \eta' - i\eta'' \quad (13)$$

$$G^*(\omega) = G' + iG'' \quad (14)$$

respectively, where  $\eta'$ ,  $G'$  are the real and  $\eta''$ ,  $G''$  are the imaginary components. The phase angle  $\delta$  is as  $\tan(\delta) = G''/G'$ . Subsequently, we review the literature pertaining to the dynamic oscillatory properties of glass fiber suspensions in non-Newtonian suspending mediums. As an introduction to each section, a brief review is given of fiber suspensions in Newtonian suspending mediums for comparison purposes. As a note, for the following section pertaining to the small-amplitude oscillatory shear flow, it can be assumed that the initial fiber orientation of the samples is random unless otherwise specified.

**(a) Complex Shear Viscosity.** There is a limited amount of published work relating to the complex viscosity of fiber-filled Newtonian fluids. The data that is published suggests only the real or viscous component of the complex viscosity exists. For short glass fiber-filled Newtonian fluids, in the *semi-dilute* and *concentrated* régime, Ganani and Powell<sup>44</sup> found the dynamic viscosity,  $\eta'$ , to be in good agreement with shear viscosity which can be seen in Fig. 2. The authors also found  $\eta'$  to remain fairly constant over a frequency range of .06-7.5 rad/s, the magnitude of which increased with fiber concentration. This behavior is similar to unfilled Newtonian fluids where the shear stress oscillates in phase with the shear rate. This suggests that though Newtonian suspensions can exhibit normal stresses, the presence of the fiber does not induce elasticity in Newtonian fluids at small strain amplitudes.

The addition of fibers to a non-Newtonian fluid increases  $|\eta^*|$ ; the degree of which is dependent on the concentration, aspect ratio and orientation distribution of the fiber.<sup>1, 46</sup> The dependence of  $|\eta^*|$  on glass fiber concentration and aspect ratio is not obvious. Many authors have published data that suggests that the addition of glass fiber has little effect on  $|\eta^*|$  when compared to the matrix material in the *dilute* and *semi-dilute* régime.<sup>1, 46, 60</sup> Guo et al.<sup>1</sup> suggested that a small amount of fiber was not sufficient to cause deviations from the properties of the neat matrix in small-amplitude oscillatory shear flow. However, in the *concentrated* régime the effects are more significant. Similar to the shear viscosity behavior at low shear rates,  $|\eta^*|$  can exhibit an enhanced Newtonian plateau<sup>1, 46</sup> or rise in an unbound manner at low frequencies.<sup>52, 60, 61</sup> At high frequencies,  $|\eta^*|$  can begin to merge onto that of the matrix<sup>52</sup> or follow a similar shear thinning curve of the matrix at a constant enhance value.<sup>1, 46</sup>

$|\eta^*|$  increasingly deviates from the shear viscosity at increasing fiber concentrations for both Newtonian and non-Newtonian fiber suspensions.<sup>1, 24, 60, 62</sup> This suggests that the Cox-Merz relationship<sup>63</sup> does not hold for glass fiber-filled systems. The Cox-Merz rule is an empiricism that states that  $|\eta^*|$  is equal to the shear viscosity at corresponding values of frequency and shear rate:<sup>64</sup>

$$\eta(\dot{\gamma}) = \left| \eta^*(\omega) \right|_{\omega=\dot{\gamma}} \quad (15)$$

Deviations from the Cox-Merz rule are typically explained by shear induced fiber orientation changes that are more prevalent in steady shear deformation than in oscillatory shear.

It is speculated that small-amplitude oscillatory shear in the linear strain region is too weak to induce fiber reorientation of the same magnitude as in steady shear flow.<sup>1</sup>  $|\eta^*|$  for a randomly oriented fiber suspension is greater than that of an aligned suspension.<sup>46</sup> For this reason,  $|\eta^*|$  of a sample with isotropic fiber orientation is typically larger than values of the shear viscosity under the same conditions and corresponding shear rates.<sup>24, 60, 62</sup> A discrepancy from this trend has been published by Guo et al.<sup>1</sup>, where at low frequencies the authors found  $|\eta^*|$  to be lower than the steady shear viscosity at corresponding frequencies and shear rates while the opposite occurred at high frequencies and shear rates for a short glass fiber-filled linear low-density polyethylene (LLDPE). However, no discussion was given about the initial fiber orientation in the samples.

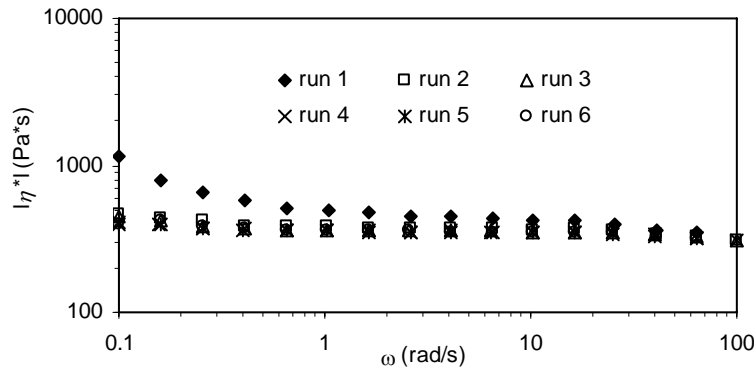


**Figure 9.** Change in  $|\eta^*|$  after repeated small-amplitude ( $\gamma_o = 0.15$ ) oscillatory tests on the same sample. Tests were performed on a short glass fiber-filled polybutylene terephthalate ( $\phi = 0.1766$ ,  $a_r \sim 21.4$ , *concentrated* régime). All tests were performed on a torsional PPR with a gap of  $\sim 2$  mm.<sup>60</sup>

Work by Kim and Song<sup>60</sup> suggests that some orientational changes do occur in dynamic oscillatory tests. They authors noticed that  $|\eta^*|$ , for a short glass fiber-filled ( $\phi = 0.1766$ ,  $a_r \sim 21.4$ , *concentrated* régime) polybutylene terephthalate (exhibits little shear rate dependence) suspension, changed after repeated dynamic oscillatory tests, Fig. 9. A sample with isotropic fiber orientation at low frequencies exhibited a yield-like behavior. After repeated tests on the same sample a Newtonian plateau developed. This suggests

that the small-amplitude shear oscillations can induce orientation in the flow direction and that the micro-structure of the fiber is a possible contributor to the yield-behavior. As a note, no comparisons were made between  $|\eta^*|$  and the steady shear viscosity for the suspension or the neat matrix.

Glass fiber suspensions in non-Newtonian fluids show a strain amplitude dependence in the dynamic functions that markedly increases with concentration and aspect ratio. Mutel and Kamal<sup>65</sup> found that the addition of short glass fibers to a PP caused a strain amplitude dependence for all concentrations tested, 10-40 wt% ( $\phi = 0.0354 - 0.1805$ ), with increasing strain amplitude dependence for increasing concentration. As a note, the neat PP suspending medium exhibited linear strain dependence through a range of 5-50 strain%. Kim and Song<sup>60</sup> found that as the strain amplitude was increased for a short glass fiber suspension, while staying in the linear strain amplitude region of the suspending medium,  $|\eta^*|$  at constant frequency decreased. This was attributed to larger strains increasing the average orientation of the fibers along the flow direction.

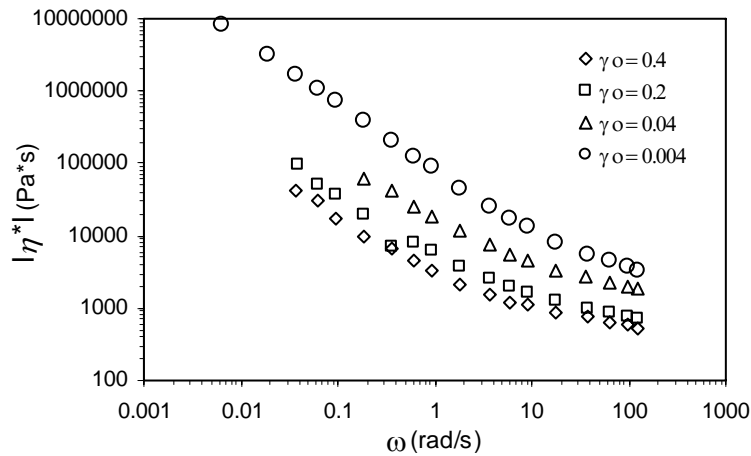
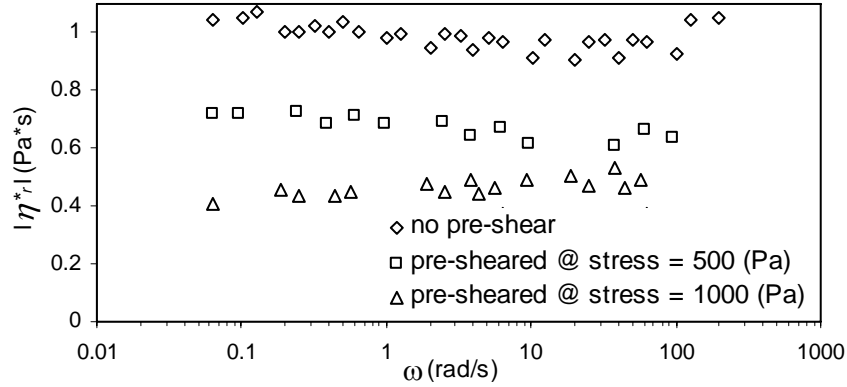


**Figure 10.**  $|\eta^*|$  vs. frequency for a long glass fiber-filled polypropylene ( $\phi = 0.132$ ,  $a_r \sim 1071$  or  $L = 15$  mm, *concentrated* régime) at various strain amplitudes  $\gamma_0$ . All tests were performed on a torsional PPR with a gap of 1mm.<sup>61</sup>

In some cases, typically with suspensions containing high glass fiber concentration and aspect ratio (relating to the *concentrated* régime), the dependence of  $|\eta^*|$  on the strain amplitude can be seen through the complete range tested, even at very low strain amplitude. The non-linear behavior at very small strain amplitudes is indicative of a yield stress and can be seen in Fig. 10, for a long glass fiber-filled polypropylene ( $\phi = 0.132$ ,  $a_r \sim 1071$  or  $L = 15$  mm, *concentrated* régime).<sup>61</sup> For this suspension  $|\eta^*|$  drastically decreases with increasing strain amplitude, even at small strains between 0.004 and 0.04 strain.

The source of the yield-like behavior exhibited by some glass fiber suspensions at high concentrations or large aspect ratios in the *concentrated* régime remains to be established. The two most plausible hypotheses are the formation of a pseudo-network between the fibers and the matrix macromolecules<sup>31</sup>, and high fiber-fiber interaction in samples with isotropic fiber orientation.<sup>60</sup> The lack of published data with regards to

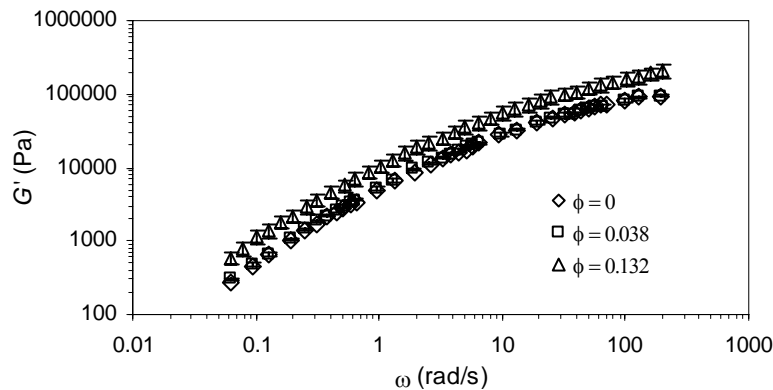
fiber surface treatments and their effect on the matrix-fiber interaction as well as the initial fiber orientation of published rheological data make it impossible to delineate the cause of the yield-like behavior.



**Figure 11.** The effects of pre-shear on  $|\eta_r^*|$  vs. frequency for a short glass fiber-filled polypropylene ( $\phi = 0.124$ ,  $a_r \sim 21.4$ , *concentrated* régime). In this case  $|\eta_r^*|$  is the pre-sheared sample normalized by the no-pre-shear sample values. All measurements were performed on a PPR.<sup>46</sup>

Similar to the shear viscosity, the initial orientation of the sample can have an effect on  $|\eta_r^*|$ . A sample whose initial orientation is random will exhibit a larger  $|\eta_r^*|$  than a sample whose fiber is oriented in the flow direction. Mobuchon et al.<sup>46</sup> reported over a 50% reduction in  $|\eta_r^*|$  after pre-shearing a *concentrated* short glass fiber-filled polypropylene ( $\phi = 0.124$ ,  $a_r \sim 21.4$ , *concentrated* régime), Fig. 11. The reduction in  $|\eta_r^*|$  was attributed to the pre-shear aligning the fibers flow direction; the greater the pre-shear stress the greater the overall fiber alignment.

**(b) Complex Shear Modulus.** There is little published data on the complex modulus or corresponding moduli of glass fiber suspensions in Newtonian fluids. Specifically, only one paper pertaining to the dynamic response of a fiber-filled purely Newtonian fluid was found. Ganani and Powell<sup>44</sup> reported that glass fiber suspensions in Newtonian fluids showed no significant values for the storage modulus  $G'$ , or no elastic behavior.



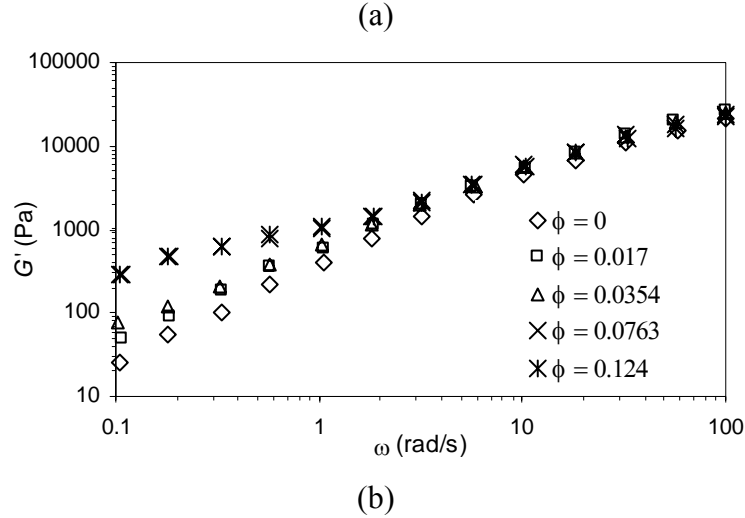


**Figure 12.** The storage modulus vs. frequency: (a) for two short glass fiber-filled polypropylene suspensions ( $\phi = 0.038$ ,  $a_r \sim 30$ , *semi-dilute* régime and  $\phi = 0.132$ ,  $a_r = 21.4$ , *concentrated* régime) and the neat suspending medium.<sup>46</sup> (b) for a short glass fiber-filled polypropylene ( $a_r = 85$  and  $35$  for  $\phi = 0.017$  and  $0.0763$  respectively, the aspect ratio for the other concentrations was not given) of various concentrations of fiber.<sup>52</sup> Both measurements were performed on a PPR.

For fiber suspensions in non-Newtonian fluids, the storage and loss modulus ( $G'$  and  $G''$ ) typically show little deviation from the neat matrix at low concentrations and small aspect ratios of fiber in the *dilute* and *semi-dilute* régimes. At high concentrations and sufficiently large aspect ratios, relating to the *concentrated* régime, two general trends become apparent. First, both the storage and loss moduli may increase in magnitude but follow the same general curve of the matrix. This trend can be seen for the storage modulus in Fig. 12 (a). Second, a more pronounced enhancement at low frequencies ( $\omega < \sim 10$  rad/s) that becomes more apparent with increasing concentration and aspect ratio. At high frequencies ( $\omega > \sim 10$  rad/s) the moduli typically merge onto the value exhibited by the matrix. This trend can be seen for  $G'$  in Fig. 12 (b). In the second case, the low frequency plateau or “tail” is indicative of a yield-like behavior and often corresponds with a  $|\eta^*|$  that does not exhibit a Newtonian plateau.<sup>52, 66</sup> The high frequency merger between the matrix and suspension moduli is typically attributed to the evolution of the fiber orientation distribution. However, no comparative studies of repeated runs or pre-shearing are reported to confirm the effect of fiber orientation on the dynamic moduli.<sup>52, 67</sup>

In all the published results that were reviewed regarding the dynamic moduli of non-Newtonian suspensions, the loss modulus was of greater magnitude than the storage modulus.<sup>1, 46, 52, 66, 67</sup> In the referenced work where the behavior of the neat resin was given for comparison purposes, the matrix also followed this trend of  $G'' > G'$ . Though the dynamic moduli can change slightly with fiber concentration and aspect ratio, the ratio of the storage and loss modulus typically remains constant.

**(c) Phase Angle.** For glass fiber suspensions in both Newtonian and non-Newtonian fluids the phase angle is independent of fiber content, and typically equal to that exhibited by the suspending fluid.<sup>53</sup> Mobuchon et al.<sup>46</sup> found the phase angle to be

independent of fiber content and fiber orientation and equal to that of the matrix over a frequency range of .1-100 rad/s for a short glass fiber-filled polypropylene. Slight deviations from this behavior do occur. Guo et al.<sup>1</sup> found that at low frequencies ( $\omega = 0.135-1.351$  rad/s)  $\tan(\delta)$  decreased with fiber volume fraction but at higher frequencies (up to 277 rad/s)  $\tan(\delta)$  remained constant with increasing fiber concentration. Similar results were published by Greene and Wilkes<sup>52</sup> for a short and long fiber-filled polypropylene.

**2.3. Transient Shear Flow.** We now consider the nonlinear viscoelastic behavior of glass fiber-filled non-Newtonian fluids in shear. The following review will include the most commonly reported experimental tests: stress growth upon inception of steady shear flow, stress relaxation after cessation of steady shear flow, interrupted stress growth and strain upon inception of constant stress. As an introduction to each section, a brief review is given to fiber suspensions in Newtonian suspending mediums for comparison purposes.

**2.3.1. Start-up of Shear Flow.** In start-up of shear flow a sample is at rest and in equilibrium when  $t < 0$ . At  $t \geq 0$  the sample is deformed with constant deformation rate while the shear stress growth function  $\sigma^+$  or corresponding shear stress growth coefficient  $\eta^+$  and the normal stress growth functions  $N_1^+$  and  $N_2^+$  are measured as a function of time and shear rate. Subsequently, we begin with a review of  $\sigma^+$  behavior followed by the normal stress growth functions of glass fiber filled non-Newtonian fluids.

**(a) Shear Stress Growth.**  $\sigma^+$ , often reported in terms of  $\eta^+$ , gives insight into the nonlinear viscoelastic behavior of glass fiber suspensions and the temporal evolution of the fibers' orientation distribution. The addition of glass fiber to a Newtonian or non-Newtonian fluid has a dramatic effect on  $\sigma^+$  in start-up of shear flow; the most profound effect being a relatively large overshoot. Initial orientation distribution, concentration and aspect ratio of the fiber, viscoelastic nature of the matrix, and the shear rate all influence the magnitude of the overshoot as well as the length of time for a steady-state to be reached.<sup>68</sup> This is speculated to be directly related to the evolving microstructure of the glass fibers within the suspension. Because the unsteady shear flow material functions are dependent on an evolving microstructure, they seem to be more affected by the presence of fiber than the steady shear flow material functions.<sup>69</sup>

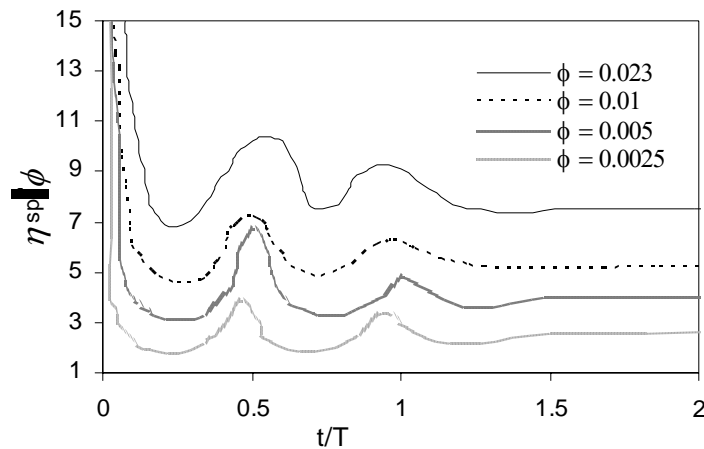


**Figure 13.** Transient specific viscosity ( $\eta_{sp} = \eta_r - 1$ ), normalized by the glass fiber

volume fraction, vs. time, normalized by the period of oscillation  $T$ . Tests were performed on a dilute suspension of rigid aluminum coated Nylon fibers of varying concentration and constant aspect ratio,  $a_r = 5.2$ , in a Newtonian suspending medium. The rods were initially aligned parallel to the direction of velocity gradient with the use of an electric field. All tests were performed on a torsional CPR, at  $\dot{\gamma} = 2.51 \text{ s}^{-1}$ .<sup>70</sup>

The transient response to deformation of a suspension is highly dependent on the Newtonian or non-Newtonian behavior of the suspending medium.<sup>33</sup> Rods in a dilute suspension whose suspending medium is a Newtonian fluid will rotate around a vorticity axis unless acted upon by another force. Mathematically described by Jeffery<sup>29</sup>, this phenomenon gives rise to an oscillating stress response that is dependent on the orientation state of the particle. In a theoretically perfect system, the period of oscillation would stay constant, but in all experimental cases the amplitude of  $\sigma^+$  decayed with time. This behavior is shown in Fig. 13 for a dilute suspension of glass fibers in a Newtonian fluid by way of the oscillating specific viscosity  $\eta_{sp}/\phi$ , normalized by the glass fiber concentration, vs. time, normalized by the period of fiber rotation. The decay of the stress oscillation can be a result of several interactions including boundary, particle-particle, hydrodynamic or slight aspect ratio variations.<sup>71</sup> For non-dilute suspensions in a Newtonian fluid, fiber-fiber and fiber-hydrodynamic interactions prevent or retard periodic fiber rotation and typically a pseudo-equilibrium orientation state is reached, which, after a short period of time, may slowly change with time.<sup>69</sup> Iso et al.<sup>47, 48</sup> performed many experiments on *dilute* and *semi-dilute* suspensions of weakly and highly elastic fluids. The authors found that the addition of a small concentration of elastic polymer lead to a competition between the spiraling toward the vorticity axis (Jeffery orbit) and the randomization of the fiber orientation due to hydrodynamic interactions. In highly elastic fluids, the authors found that the polymer stress acted to confine the fiber orientation to the flow direction. In both cases the behavior was attributed to the elastic stresses competing with hydrodynamic forces.

Ganani and Powell<sup>44</sup> performed start-up of shear flow experiments on fiber suspensions in Newtonian fluids in the *concentrated* régime ( $\phi = 0.08$ ,  $a_r = 24.3$ , tests performed on a CPR). They found that the suspensions exhibit stress shear growth functions similar to viscoelastic suspensions. Upon flow, a sample that started with a random orientation state would exhibit a peak in the stress overshoot of roughly 25% greater than the steady-state value. The overshoot maximum occurred at a strain of roughly 5, and completely decayed by a strain of roughly 15.

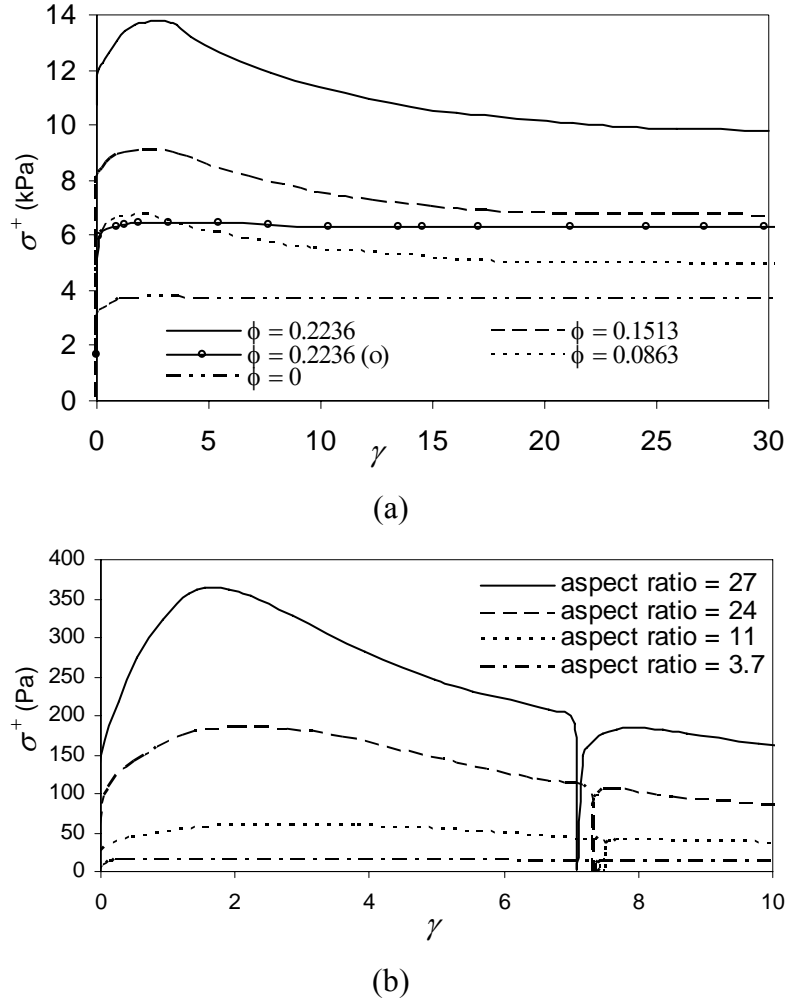


**Figure 14.**  $\sigma^+$  vs. strain. All tests were performed on a CPR. (a) Polystyrene-acrylonitrile (SAN, estimated density  $\approx 1.4 \text{ g/cm}^3$ ) containing short glass fibers ( $a_r = 22$ ) of varying concentrations (*concentrated* régime) and one sample containing glass beads denoted by (o) with diameter of 3-5  $\mu\text{m}$ . Experiments were performed at a shear rate of  $0.2 \text{ s}^{-1}$ . (b) Polyamid-6 (Nylon-6) containing short glass fibers of constant concentration ( $\phi = 0.1507$ ) and varying aspect ratio. The smallest aspect ratio sample was in the *semi-dilute* régime, and the rest were *concentrated*. The experiments were performed at  $\dot{\gamma} = 0.1 \text{ s}^{-1}$  that was interrupted at  $\gamma \sim 7$ .<sup>33</sup>

Unlike glass fiber suspensions in Newtonian fluids,  $\sigma^+$  of suspensions in non-Newtonian fluids does not oscillate at very dilute fiber concentrations and small aspect ratios, but rises to a peak that decays to a steady-state (stress overshoot) or simply rises to a steady-state value.<sup>47, 48</sup> The effect of glass fibers on  $\sigma^+$  is primarily quantified by the magnitude of stress overshoot. Increasing fiber concentration and/or fiber aspect ratio increases the overshoot and the time needed to reach steady-state in a similar manner. Fig. 14 (a) is a graph of  $\sigma^+$  vs. strain for a polystyrene-acrylonitrile (SAN, estimated density  $\approx 1.4 \text{ g/cm}^3$ ) containing short glass fibers ( $a_r = 22$ ) of varying concentrations (all in the *concentrated* régime) and one sample containing glass beads with diameters

between 3-5  $\mu\text{m}$ . It is interesting to note the effect of glass spheres on the rheology in comparison to glass fibers at similar concentrations, in Fig. 14 (a). First, the suspension containing glass spheres does not exhibit any visible shear stress overshoot but does enhance the steady state stress by roughly 50%. Second, the presence of glass fibers enhanced the steady state shear stress of the suspending medium by roughly 80% more than does the presence of glass spheres. This suggests that the stress overshoot is a result of the evolving fiber orientation and that the glass fibers are restricted from completely aligning in the flow direction. Fig. 14 (b) is a graph of  $\sigma^+$  vs. strain for a polyamid-6 (Nylon-6) containing short glass fibers of constant concentration ( $\phi = 0.1507$ ) and varying aspect ratio. The smallest aspect ratio sample was in the *semi-dilute* régime, and the rest were in the *concentrated* régime. The experiment was interrupted at a strain  $\gamma \sim 7$ , the results of which will be discussed later in the appropriate section. Similar to increasing the fiber concentration, increasing the fiber aspect ratio increased the magnitude of the stress overshoot and the steady-state stress.

The overshoot in Newtonian and non-Newtonian suspensions is speculated to be a result of an evolving microstructure, where, upon flow the fibers orient themselves towards the flow direction. A sample whose initial fiber orientation is aligned parallel to the direction of velocity gradient will exhibit the greatest overshoot. In contrast, a sample whose initial fiber orientation is parallel to the flow direction will exhibit the lowest overshoot, with a randomly oriented sample falling between these two ideal cases.<sup>33</sup> Ramazani et al.<sup>69</sup> showed that pre-shearing a sample before the stress growth experiments removed the initial overshoot exhibited by randomly oriented fiber suspensions. The peak of the shear stress overshoot scales with strain at varying shear rates and typically occurs between 2-10 strain units. Current theory suggest that the peak in the shear stress overshoot corresponds to an average fiber orientation of  $45^\circ$  with respect to the flow direction.<sup>33, 69</sup> However, no thorough experimental analysis to confirm the orientation distribution that coincides with a specific stress response has been reported. A steady-state in the stresses can be reached if ample time is given for a suspensions' fiber orientation to reach a steady-state at that given shear rate, which typically occurs at 50-100 strain units.<sup>30</sup>

There is an insufficient amount of comparable data to delineate the effect of matrix viscosity and elasticity on  $\sigma^+$  of glass fiber suspensions in non-Newtonian fluids. However, upon reviewing the current published transient data it would appear that the magnitude of the initial overshoot increases with increasing matrix elasticity, interfacial matrix-fiber interaction and viscosity; with the viscosity being a secondary factor to the matrix elasticity and matrix-fiber interaction.<sup>11, 31, 39</sup> A simple experiment, that to our knowledge has not been reported with respect to stress growth functions, would be to run start-up of shear flow tests on similar samples at various temperatures, effectively changing the viscosity of the suspending medium. This would help elucidate the effect of suspending medium viscosity on the stress overshoot and corresponding evolution of the fiber orientation.

**(b) First and Second Normal Stress Growth Functions.** The published rheological data pertaining to the normal stress growth functions of glass fiber suspensions in Newtonian fluids is limited. However, the response of Newtonian-like suspensions (i.e. polybutene) suggests that the presence of fiber does induce normal stresses that exhibit transient behavior in Newtonian fluids. For non-Newtonian

suspensions, similar to  $\sigma^+$ , the magnitude of  $N_1^+$  or  $N_1^+ - N_2^+$  overshoot increases with increasing concentration, aspect ratio, and shear rate.<sup>33, 68</sup> The peak in the overshoot can be as large as an order of magnitude greater than the steady-state value.<sup>31, 68, 69</sup> The overshoot scales with strain at various shear rates and the peak of the overshoot typically occurs at a greater strain than the shear stress overshoot. As previously discussed, it has been suggested that the peak of the shear stress growth overshoot relates to an average fiber orientation of  $45^\circ$  with the flow direction.

**2.3.2. Cessation of Steady Shear Flow.** The stress relaxation experiment is defined so that a sample at  $t < 0$  is subject to steady shear flow and at steady state. At  $t \geq 0$  the flow is stopped and the shear stress decay function  $\sigma^-$ , and the normal stress decay functions  $N_1^-$  and  $N_2^-$  are measured as a function of time and shear rate. Subsequently, we begin with a review of the shear stress decay function behavior followed by the normal stress decay functions of glass fiber filled non-Newtonian fluids.

**(a) Shear Stress Decay.** In Newtonian suspensions the presence of fiber has little effect on shear stress decay function behavior.<sup>2</sup> Likewise, with non-Newtonian suspensions it is typically stated that the presence of the fibers has a negligible influence on the relaxation dynamics of a suspension when compared to the neat matrix.<sup>31, 33, 68</sup> Laun<sup>33</sup> showed that an increase in fiber concentration had negligible effect on the time needed for half the steady-state stress to relax which was concluded from the data plotted in Fig. 14 (a) for a polystyrene-acrylonitrile (SAN) containing short glass fibers ( $a_r = 22$ ) of varying concentrations (all in the *concentrated* régime).

**(b) Normal Stress Decay.** Similar to the normal stress growth functions, there is little data pertaining to the normal stress decay function of glass fiber suspensions in Newtonian fluids. However, the response of suspensions whose suspending mediums are Newtonian-like (i.e. polybutene) suggests that the presence of fiber has little effect on the relaxation behavior.<sup>31</sup> The same is true for non-Newtonian suspensions. Similar to the stress relaxation, it is typically stated that the presence of fiber has little impact on the relaxation behavior of the normal stress differences.<sup>33, 68</sup> Laun<sup>33</sup> found no difference in the time for  $N_1^- - N_2^-$  to relax to half its steady state value, for concentrations between 0 and 35wt% ( $\phi \sim 0-0.2236$ ) of short glass fiber in SAN.

**2.3.3. Interrupted Shear Flow.** Interrupted stress growth experiments are designed such that a sample is deformed at a constant shear rate for a specific time, after which the flow is stopped. Then the flow is turned back on, either immediately or after a pre-determined period of time, in the same flow direction or the reverse direction (flow reversal tests). Because the initial response of a suspension is exactly the same as described in the preceding sections, we will focus our discussion on the stress growth behavior of the suspension after the flow is reapplied to the suspension.

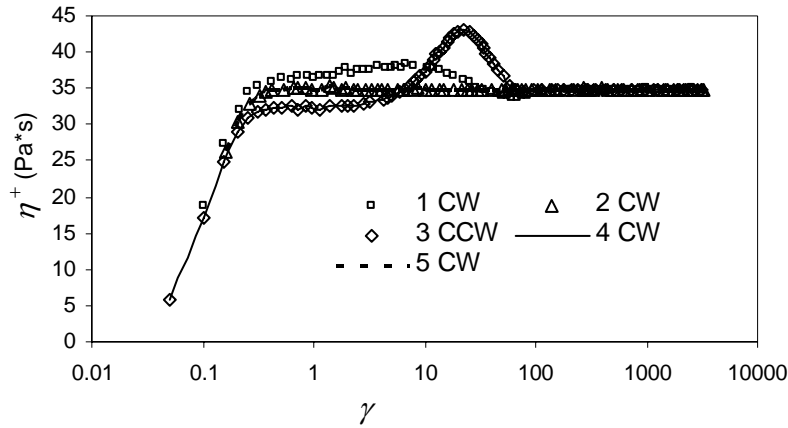
The effect of fiber concentration and aspect ratio on interrupted experiments is similar in nature to the stress growth and relaxation experiments reviewed in the preceding sections. The following section on interrupted stress growth is meant to further the reader's understanding of how various flow conditions and shear histories can have an effect on the rheological behavior. The review begins with the interrupted shear stress growth behavior of Newtonian and non-Newtonian suspensions followed by the behavior of the shear stress in flow reversal. Then we review the normal stress differences with the same format.

**(a) Shear Stress Growth.** We first consider the case of a glass fiber suspension in a Newtonian fluid that has been subject to an interrupted shear flow experiment where the flow is reapplied in the same direction as the initial flow. Ganani and Powell<sup>2</sup> showed for a *semi-dilute* short glass fiber-filled Newtonian fluid ( $\phi = 0.08$ ,  $a_r = 24.3$ , tests performed on a CPR) that when the flow was reapplied after a wait period of one minute the shear stress rose immediately to the steady-state value. However, when the sample was allowed to rest for a greater period of time  $\sim 10$  minutes, the overshoot reappeared with similar magnitude to the first deformation. The behavior was attributed to particle sedimentation, altering the steady-state fiber orientation distribution resulting in a change in the fibers orientation distribution when the flow was reapplied. This hypothesis can be supported with the use of Eq. (9) that estimates the time scale for sedimentation of the fibers and is found to be  $\sim 10$  min, assuming a low suspending medium viscosity of  $\eta_s \sim 2$  Pa\*s and a fluid density of  $1 \text{ g/cm}^3$ .

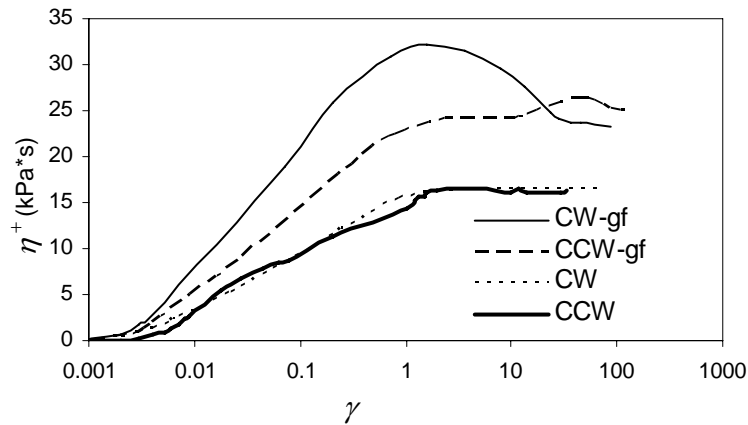
The shear stress response to flow reversal tests, for the same suspension described in the paragraph above, was slightly different. Only a one minute rest time after the flow was removed from the sample was needed for an overshoot of similar magnitude to the initial overshoot to appear in the reverse direction. Again, this was attributed to particle sedimentation. However, no comment was made on why the suspension assumed a new orientation distribution after only one minute in the reverse direction while it took  $\sim 10$  minutes of rest for the overshoot to reappear in the same flow direction.

We now consider the shear stress response to interrupted flow of non-Newtonian fluids containing glass fibers. Fig. 14 (b) is a typical example where after the sample is subject to start-up of shear flow, the flow is stopped and then immediately reapplied in the same direction. As expected  $\sigma^+$  momentarily relaxes as the flow is interrupted and then returns to the previous value.<sup>33</sup> The lack of an overshoot peak on resumption of flow was attributed to the lack of any recovery of orientation and structure during the period of no flow. This is a typical response for viscoelastic fluids where sedimentation and Brownian motion are not contributing factors even after very long interruptions of flow, though deviations from this behavior do occur.<sup>30</sup> For example, when an overshoot reappears during interrupted tests with long interruption times between flow in the same direction. There is debate on the cause of this phenomenon, but one common factor between the suspensions that exhibited this response was they had low viscosity suspending mediums which suggests the possibility of particle sedimentation altering flow induced fiber orientation at least slightly during quiescent rest periods.<sup>3</sup> However, Sepehr et al.<sup>31</sup> explained this behavior exhibited by a Boger fluid suspension by the elastic recoil of the macromolecules altering the fiber orientation during stress relaxation.  $\sigma^+$  in flow reversal experiments, when the flow is re-applied in the opposite direction as the initial deformation, exhibits a slightly more complex behavior. When  $\sigma^+$  is plotted vs.  $\ln(\dot{\gamma})$  it is first seen to rise to a pseudo plateau which is explained in the following way. In concentrated suspensions the fibers orient in the flow direction and form a “crystalline” structure of least resistance to flow. When the flow is reversed the aligned microstructure has a low resistance to flow until it tilts over in the new flow direction to form its mirror image. The reverse overshoot is a result of the reverse tumbling of the fibers, even if the fibers were aligned prior to flow reversal. The peak of the reverse overshoot occurs at an increased strain compared to the first overshoot and increases with concentration and aspect ratio and the overshoot peak scales with strain.<sup>31, 44</sup>

Interestingly, Sepehr et al.<sup>31</sup> found that the magnitude of the reverse overshoot in Newtonian and non-Newtonian suspensions decreases with increasing  $\dot{\gamma}$ , but no explanation to why was given by the authors. One possible explanation, which correlates with rheological data shown previously, is that higher shear rates impart a higher degree of orientation at steady state. As a result, fewer fibers are subject to tilt or rotation during flow reversal with increasing shear rates.



(a)



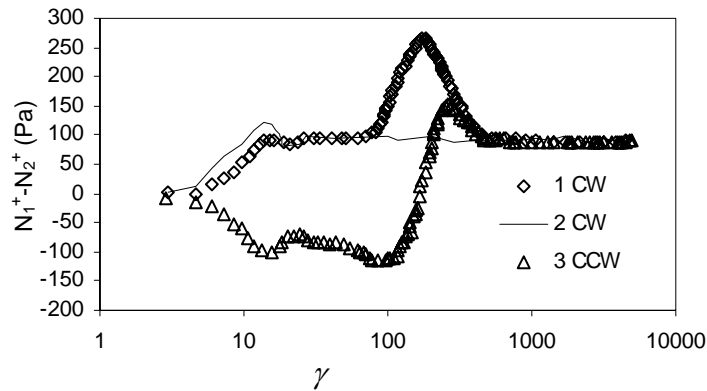
(b)

**Figure 15.**  $\eta^+$  vs. strain for interrupted stress growth tests. All tests were performed on a torsional PPR with gap-to-fiber length ratio greater than 3:1. The clockwise (CW) and counter clockwise (CCW) notation is to give the reader context of the shear direction in a torsional rheometer. The flow reversal was applied immediately to the sample. (a) Short glass fiber-filled polybutene PB (fiber content:  $\phi = 0.0706$ ,  $a_r \sim 20$ , *concentrated*) suspension at  $\dot{\gamma} = 5 \text{ s}^{-1}$ .<sup>31</sup> (b) Neat and short glass fiber-filled polypropylene PP (fiber content:  $\phi = 0.115$ ,  $a_r \sim 20$ , *concentrated*), denoted in the figure as -gf, at  $\dot{\gamma} = 0.1 \text{ s}^{-1}$ .<sup>68</sup>

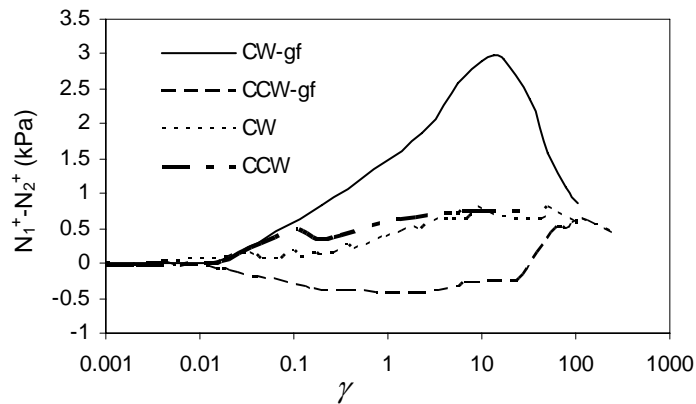
Results of the flow reversal test can be seen in Fig. 15 (a) and (b) for a short glass fiber-filled polybutene (glass content:  $\phi = 0.0706$ ,  $a_r \sim 20$ ) and a short glass fiber-filled polypropylene (fiber content:  $\phi = 0.115$ ,  $a_r \sim 21$ ), respectively. For the polybutene suspension, the weak initial overshoot compared to the reverse overshoot is most likely

due to orientation distribution of fiber generated during sample loading into the rheometer. An interesting observation is that the reverse overshoot for the polybutene (Newtonian-like) suspension is greater in magnitude than the first overshoot, as seen in Fig. 15 (a), but for the polypropylene (non-Newtonian) suspension the second overshoot is smaller, as seen in Fig. 15 (b). It is difficult to draw a precise conclusion from comparing these two graphs as the tests were performed at different shear rates, but a possible explanation for this behavior can be established through the work of Iso et al.<sup>47, 48</sup> He found that the elastic nature of non-Newtonian fluids stabilizes fiber rotation. This could result in a greater number of fibers tumbling  $180^\circ$  in the Newtonian suspensions when compared to the non-Newtonian suspensions.

**(b) Interrupted Normal Stress Growth Function.** We now consider  $N_1^+$  in interrupted flow and flow reversal experiments. For a short glass fiber-filled polybutene (PB) suspension starting with an isotropic fiber orientation, Sepehr et al.<sup>31</sup> found that  $N_1^+ - N_2^+$ , on a  $N_1^+ - N_2^+$  vs.  $\ln(\gamma)$  plot to initially rise to a plateau equal to that of the steady-state value before exhibiting a large overshoot. The peak of the initial overshoot occurred at a strain of roughly 100, Fig. 16 (a). In Fig. 16 (a), 1<sup>st</sup> CW is the initial deformation in the clockwise direction starting from a random fiber orientation. 2<sup>nd</sup> CW is an intermittent deformation in the same clockwise direction. As expected during the 2<sup>nd</sup> CW the overshoot is no longer present. However, in the 3<sup>rd</sup> deformation in the CCW (counter clockwise) direction the normal stress initially takes on a negative value before rising to an overshoot corresponding to a similar strain seen in the first overshoot.



(a)



(b)

**Figure 16.**  $N_1^+ - N_2^+$  plotted vs. strain. All tests were performed on torsional PPR with gap-to-fiber length ratio greater than 3:1. The clockwise (CW) and counter clockwise (CCW) notation denotes the direction of plate rotation. The flow reversal was applied immediately to the sample. (a) Short glass fiber-filled polybutene PB (fiber content:  $\phi = 0.0706$ ,  $a_r \sim 20$ , *concentrated*) suspension at  $\dot{\gamma} = 5 \text{ s}^{-1}$ .<sup>31</sup> (b) Neat and short glass fiber-filled polypropylene PP (fiber content:  $\phi = 0.115$ ,  $a_r \sim 20$ , *concentrated*), denoted in the figure as -gf, at  $\dot{\gamma} = 0.1 \text{ s}^{-1}$ .<sup>68</sup>

Suspensions whose matrix have elastic properties and exhibit a large degree of shear rate dependence have been shown to behave similarly to the previously described polybutene suspension.<sup>31, 68, 69</sup> In Fig. 16 (b)  $N_1^+ - N_2^+$  is shown for a short glass fiber-filled polypropylene, PP30, and the neat polypropylene, PP0, for comparison.<sup>68</sup> Starting from an isotropic fiber orientation, the sample exhibits a large overshoot but does not have the initial plateau exhibited by the polybutene suspension. However, it does exhibit the negative  $N_1^+ - N_2^+$  when the flow is reversed. The authors hypothesize that the cause of the negative normal stress differences is due to non-affine deformation similar to liquid-crystalline polymers.<sup>68</sup>

**2.3.4. Creep.** In creep experiments a sample is subject to a constant stress and the strain is recorded. The following is a review of literature pertaining to this experiment with regard to non-Newtonian suspensions as no experimental data was found with regard to Newtonian suspensions.

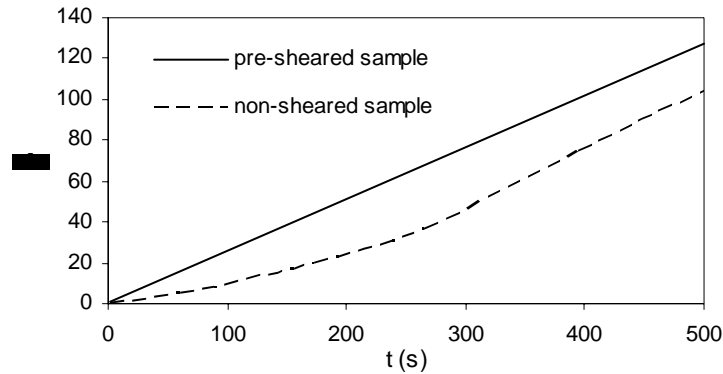


**Figure 17.** Strain vs. time for a short glass fiber-filled ( $a_r = 25$ ,  $\phi = 0.124$ , *concentrated*) polypropylene subject to a shear stress of 400 Pa; experiments were performed on a torsional PPR.<sup>72</sup>

Using a sliding plate rheometer Laun<sup>33</sup> studied the creep behavior of a short glass fiber-filled LDPE ( $a_r = 31$ ,  $\phi = 0.131$ ) with different initial fiber orientations of random, in the shear plane and parallel to the direction of velocity gradient. He found that fibers oriented in the flow direction exhibited the least resistance. Interestingly, the slope of the creep curve for fibers oriented in the shear plane but perpendicular to the flow was only slightly lower. The highest resistance was found in samples whose fiber orientation was parallel to the direction of velocity gradient. The resistance to flow of a randomly

oriented sample was found to lie between these two ideal cases. The effect of fiber orientation on the creep behavior of a short glass fiber-filled polypropylene ( $a_r = 25$ ,  $\phi = 0.124$ ) subject to a shear stress of 400 Pa can be seen in Fig. 17. The pre-sheared sample exhibits a greater slope, lower creep viscosity, than the non-sheared sample at short times while at  $t > 250$  (s) they seem to become equal. This is attributed to the fibers aligning themselves in the flow direction.

### 3. Extensional Rheology

The majority of the published work relating to the rheological behavior of glass fiber suspensions has been concerned with shear flows. This is for two reasons: first, shear flows can dominate the kinematics in extrusion and other processing flow fields and second, obtaining reliable and reproducible data in extension is difficult. However, in the frontal region of mold filling and in converging or diverging flow situations extensional behavior is important.

In the case where  $\dot{\epsilon}$  is the largest principle strain rate then the strain rate tensor takes the following form,<sup>43</sup>

$$\dot{\epsilon} = \begin{bmatrix} 1 & 0 & 0 \\ 0 & m & 0 \\ 0 & 0 & -(1+m) \end{bmatrix} \quad (16)$$

where every possible extensional flow corresponds to some value for  $m$  between -0.5 and +1.0. The extensional flows of interest here are tensile, biaxial and planar corresponding to values for  $m = -1/2$ , 1 and 0 respectively. The tensile, biaxial and planar elongational stress growth coefficient (transient elongational viscosity)  $\eta_E^+$ ,  $\eta_B^+$ , and  $\eta_P^+$  respectively are defined generally through the following relation,

$$\eta^+ = \underline{\sigma}_1^+ / \dot{\epsilon} \quad (19)$$

where  $\underline{\sigma}_1^+ = \sigma_{11}^+ - \sigma_{22}^+$  is the first normal stress growth function and is dependent on both strain rate and time. The steady state elongational viscosity  $\eta_E$ ,  $\eta_B$ , and  $\eta_P$  denotes the value of the elongational stress growth coefficient when the first normal stress growth has reached a steady state. Subsequently, we review the literature pertaining to the shear-free flow rheological behavior of glass fiber suspensions, first with tensile extension kinematics followed by biaxial extension and then planar.

**3.1. Tensile Extension.** The tensile viscosity of glass fiber suspensions in Newtonian fluids is enhanced by the presence of glass fiber but is typically reported to be independent of the strain rate.<sup>3</sup> The degree of the tensile viscosity enhancement is a function of both concentration and aspect ratio and can be more than an order of magnitude greater than the tensile viscosity of the suspending medium. Even more interesting is the ratio of the tensile viscosity to the shear viscosity, termed the Trouton ratio. For Newtonian fluids and non-Newtonian fluids that tend toward linear viscoelastic behavior at small strain and shear rates the ratio is typically equal to three. Mewis and Metzner<sup>73</sup> found a constant tensile viscosity, that exhibited no strain

thickening behavior, for glass fiber suspensions of various fiber aspect ratios ( $a_r = 280$ -1260) in a Newtonian fluid that was between one and two orders of magnitude greater than the shear viscosity. Weinberger and Goddard<sup>74</sup> found that the extensional kinematics caused quick fiber alignment resulting in a constant tensile viscosity that was roughly 26 times greater than the shear viscosity.

The shear-free flow behavior of glass fiber suspensions in non-Newtonian fluids is more interesting. The tensile viscosity increases with increasing fiber concentration and aspect ratio, but the fibers induce a strain rate thinning behavior. Using a Rheometrics Elongational Rheometer (RER), Kamal et al.<sup>75</sup> reported tensile viscosity data for a glass fiber-filled polypropylene with varying concentration (fiber content:  $\phi = 0$ -0.1805,  $a_r = 150$ ) at strain rates of 0.003-0.6  $s^{-1}$ . The authors found that the tensile viscosity increased with an increase in fiber concentration, but decreased with increasing strain rate. As a note, the neat polypropylene matrix exhibited an increasing tensile viscosity with increasing strain rate. The strain rate thinning behavior was believed to be a result of an induced shear flow between the filler particles, which increase with fiber concentration. Similar results have been published by Chan et al.<sup>59</sup> for short glass fibers in high-density polyethylene HDPE and Creasy and Advani<sup>76</sup> for a long discontinuous carbon fiber-filled poly-ether-ketone. Both studies were performed on an elongational rheometer that was built “in-lab”.

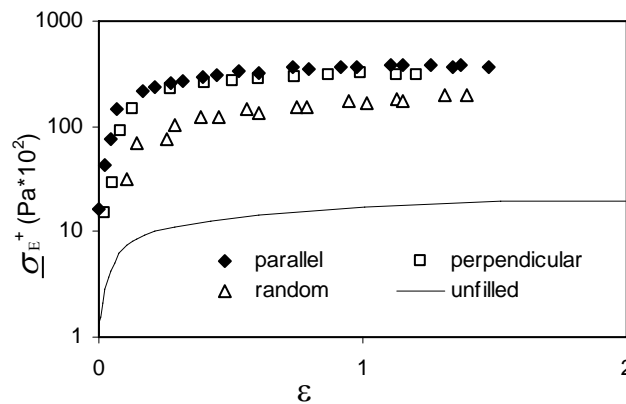
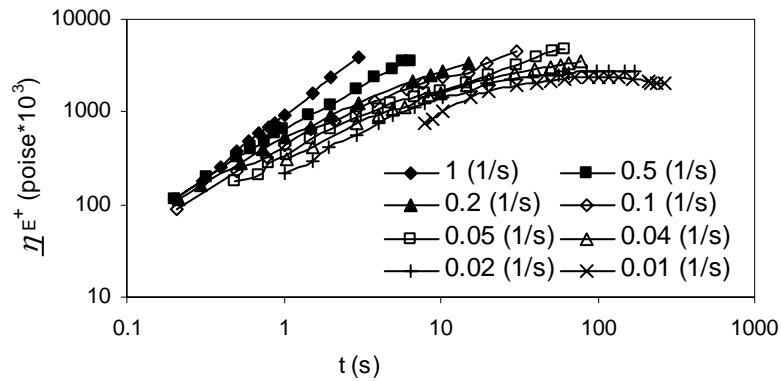


**Figure 18.** Tensile stress growth function vs. strain,  $\epsilon = L/L_0$ , for a short glass fiber filled high-density polyethylene HDPE (fiber content:  $\phi = 0.1358$ ,  $a_r \sim 30$ , *concentrated*) with various initial fiber orientations. The samples were prepared from compression molded and injection molded plates. Experiments were performed at a strain rate of 0.1  $s^{-1}$  on a Meissner type extensional rheometer.<sup>33</sup>

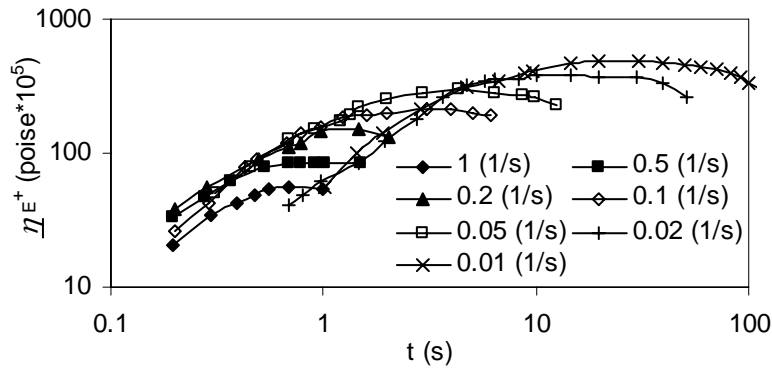
Similar to glass fiber-filled Newtonian fluids, glass fiber-filled non-Newtonian fluids can exhibit tensile stresses over an order of magnitude greater than that exhibited by the suspending medium. Laun<sup>33</sup> found the tensile viscosity for a short glass fiber-filled HDPE (fiber content:  $\phi = 0.1358$ , aspect ratio  $\sim 30$ ) to be 46 times greater than the neat suspending medium (tests were performed on a Meissner type elongational rheometer). Using the same HDPE suspension Laun compared the extensional behavior of samples with different initial fiber orientations of parallel and perpendicular to the direction of elongation and random, Fig. 18. The shape of the tensile stress growth

function was similar to the neat suspending medium for all samples but the sample whose fibers were aligned parallel to the direction of elongation exhibited the greatest tensile stress values, even after a steady state was reached.

Some researchers have attempted to approximate the tensile viscosity. Using both the approximation by Binding<sup>77</sup> and by Cogswell<sup>78</sup>, Thomasset et al.<sup>61</sup> calculated the apparent tensile viscosity from the pressure loss in a conical capillary entrance. The authors found that both methods gave similar results. For a long glass fiber-filled polypropylene (fiber content:  $\phi = 0.076-0.18$ ,  $a_r = 714-1428$  pre-extrusion), the tensile viscosity increased with fiber concentration and aspect ratio. However, the shape of the curve remained constant and followed the shear thinning behavior exhibited by the shear viscosity. This was expected as the Bagley corrections were found to be independent of shear rate. Also, the Trouton ratio increased with fiber concentration and aspect ratio from six for the neat resin to 23 for the highest concentration suspension.



(a)



(b)

**Figure 19.** Tensile stress growth coefficient vs. time. Experiments in both graphs were completed on an in-house built fiber extensional rheometer. (a) Neat polystyrene at various strain rates. (b) Short glass fiber-filled polystyrene (fiber content:  $\phi = 0.0872$ ,  $a_r \sim 140$ , *concentrated*) at various strain rates.<sup>59</sup>

Most transient extensional rheology studies for non-Newtonian suspensions focus on the effect fibers have on the time-dependent tensile stress growth coefficient, or the biaxial stress growth coefficient plotted vs. time or Hencky strain.<sup>75, 76, 79, 80</sup> These tests

suggest that the presence of fibers suppresses the strain thickening behavior of the suspending medium.<sup>79</sup> The tensile stress growth coefficient can be seen in Fig. 19 for a neat polystyrene (PS), Fig. 19 (a), and a short glass fiber-filled PS (fiber content:  $\phi = 0.091$ ) Fig. 19 (b). The fiber-filled suspension, when compared to the neat resin, seems to suppress the strain thickening characteristics of the melt.

**3.2. Biaxial Extension.** The literature pertaining to biaxial extension of glass fiber suspension is limited. However, the published data that was found suggests a similar trend to that seen in tensile extension, the presence of glass fiber enhances the biaxial viscosity but suppresses the biaxial strain thickening characteristics of the suspending medium.

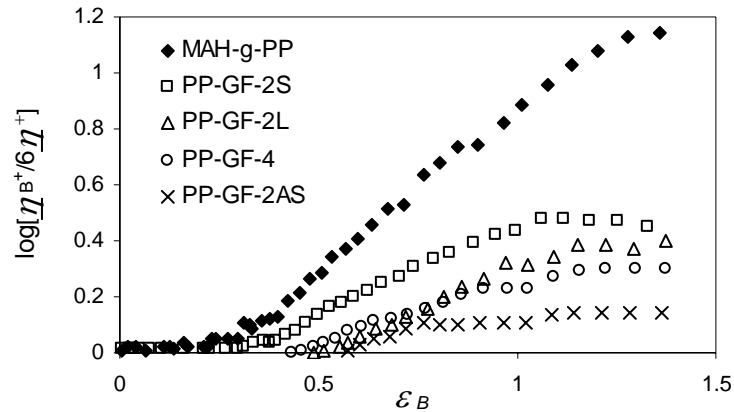


**Figure 20.** Biaxial stress growth coefficient normalized by six times the shear stress growth coefficient vs. biaxial strain for a neat maleic anhydride modified polypropylene (MAH-g-PP) and four fiber-filled suspensions of various fiber content. Three of the glass fiber filled samples were composed of a similar MAH modified PP suspending medium as the neat fluid denoted PP/GF-2S (fiber content:  $\phi = 0.0763$ ,  $a_r \sim 24.4$ ), PP/GF-2L (fiber content:  $\phi = 0.0763$ ,  $a_r \sim 36.4$ ), PP/GF-4 (fiber content:  $\phi = 0.1805$ ,  $a_r \sim 28.4$ ) and one glass fiber filled sample was composed of an unmodified PP suspending medium denoted as PP/GF-2AS (fiber content:  $\phi = 0.0763$ ,  $a_r \sim 50$ ). All samples were all in the *concentrated* régime. Experiments were performed at a biaxial strain rate of  $\sim 0.04 \text{ s}^{-1}$ .<sup>79</sup>

The effect of glass fiber on the biaxial strain thickening can be seen in Fig. 20. Fig. 20 depicts the biaxial stress growth coefficient normalized by six times the shear stress growth coefficient of the corresponding fluid vs. biaxial strain for a neat maleic anhydride modified polypropylene (MAH-PP) and four short glass fiber-filled MAH-PP samples. The ratio of the biaxial viscosity to the shear viscosity is six in the linear viscoelastic region. The neat MAH-PP showed the greatest strain hardening effects which decreased with increasing fiber concentration and aspect ratio of fiber. The weakest strain thickening occurred in the glass fiber suspension which had no MAH modification. This suggests that the interaction between the fiber and the matrix influences the strain hardening behavior.

**3.3. Planar Extension.** No literature pertaining to the direct measurement of glass fiber suspensions in planar elongation was found. However, Mobuchon et al.<sup>46</sup> developed a novel on-line slit rheometer attached to an injection molder to study shear

rheology and apparent  $\eta_p$  of glass fiber suspensions under injection molding conditions. The apparent  $\eta_p$  was found by measuring the pressure drop over the planer converging region combined with the Binding<sup>77</sup> and Cogswell<sup>78</sup> approximations. Using this approach a short glass fiber-filled polypropylene exhibited a Trouton ratio of around 40 for low extension rates ( $0.2 \text{ s}^{-1}$ ) that decreased to roughly 4 at high extension rates ( $200 \text{ s}^{-1}$ ). The authors found that an increase in concentration ( $\phi = 0.035\text{-}0.124$ ) had little effect on the  $\eta_p$  when compared to the neat suspending medium.

## 4. Flow Phenomena

**4.1. Weissenberg Effect.** When a rotating rod comes in contact with a viscoelastic fluid the meniscus will climb the rod. This effect is known as the Weissenberg effect and is typically attributed to normal stresses within a fluid. Because normal stresses must be present, homogeneous Newtonian fluids do not exhibit this behavior. However many authors have observed rod climbing by fiber-filled Newtonian fluid suspensions that exhibit little elastic behavior through a measure of  $G'$  but exhibit normal stresses.<sup>3, 25, 59, 73</sup> Chan et al.<sup>59</sup> explained this behavior by the shear flow of the suspending medium between the fibers inducing a tensile stress which act along the streamlines creating a normal force. Others attributed normal forces and hence, rod-climbing, to fiber-fiber interactions.<sup>3</sup>

**4.2. Entrance Pressure Loss.** The entrance pressure loss through a contraction is of interest to many researchers, primary because it has been suggested that it is related to the tensile viscosity of a fluid. Both the entrance and exit pressure loss increases with fiber concentration and aspect ratio.<sup>1, 33, 61</sup> Guo et al.<sup>1</sup> found the exit pressure drop to increase with fiber concentration up to  $\phi = 0.3$ . The authors also reported that increasing fiber aspect ratio had a more pronounced effect on the exit pressure drop than the shear and complex viscosities. Laun<sup>33</sup> found that the entrance pressure loss increased with the addition of fibers and was independent of melt temperature, i.e. viscosity for both a low-density and high-density polyethylene (LDPE:  $\phi = 0.131$ ,  $a_r \sim 31$ ; HDPE:  $\phi = 0.136$ ,  $a_r \sim 30$ ). Thomasset et al.<sup>61</sup> found similar results for long glass fiber suspensions that were independent of capillary diameter. The increase in pressure loss at the entrance and exit is attributed to the random fiber orientation in the barrel of the capillary rheometer rotating to align in the flow direction at the capillary entrance. However, there are no studies that investigate the effect of fiber orientation within the barrel of the capillary and its possible effects on the steady shear material functions or entrance pressure.

**4.3. Extrudate Swell.** Extrudate swell is a processing phenomenon that can occur during the extrusion process through any die geometry.<sup>38</sup> For viscoelastic fluids, extrudate swell is thought to be associated with the elastic component or normal stresses within the fluid and most empirical equations that attempt to predict the amount of extrudate swell as a function of shear rate, have a non-zero  $N_1$ .<sup>51</sup> The presence of fibers significantly reduces the amount of extrudate swell, compared to the neat matrix and introduces gross surface irregularities, especially at low shear rates.<sup>38</sup> Becraft and Metzner<sup>38</sup> found that for glass fiber-filled polypropylene suspensions (fiber content:  $\phi = 0.0369, 0.187$  and  $a_r \sim 64, 27$  respectively), filaments that were extruded below a shear rate of  $\sim 115 \text{ s}^{-1}$  (shear rate is below that associated with melt fracture) had irregular diameters and a “fuzzy” surface. The fuzzy surface appearance was a result of fibers

protruding from the surface of the filament. It was hypothesized that the somewhat flexible fibers traveled through the capillary in a bent position. The fibers closest to the surface were then able to “spring out” after exiting the die. Kalaprasad et al.<sup>39</sup> found a 20% reduction of die swell when short glass fibers were added to a low-density polyethylene. Similar results for diameter and surface irregularities have been published by Wu<sup>37</sup>, Crowson et al.<sup>81</sup>, and Knuttson and White<sup>82</sup>. The apparent contradiction between the increased normal stress differences but decreased extrudate swell is unclear.

## 5. Summary on the Rheology of Fiber Suspensions

Adding fibers to either a Newtonian or non-Newtonian fluid can have a dramatic effect on both the shear and shear-free flow rheological behavior of that fluid. The extent and magnitude of the effect is a function of the fiber’s orientation distribution, concentration, aspect ratio, suspending medium’s viscoelastic properties and interaction with the suspending medium. The effect of the glass fiber on the rheology is greatest in the case of an evolving microstructure. This is a direct result of a change in the characteristic length of a fiber depending on its orientation relative to the direction of flow.

Careful consideration should be taken by any perspective researcher to the rheometric device used to characterize glass fiber suspensions as the geometry may influence the results. In addition, it would be invaluable for researchers to either pre-condition or experimentally determine the initial orientation distribution of suspension samples. This would aid in delineating the effects of the fiber on the rheology, especially with respect to experiments associated with the linear and non-linear viscoelasticity in shear and non-linear viscoelasticity in extension.

Some of the interesting effects that glass fibers can have on the steady shear flow rheology are increased yield-like behavior and the onset of shear thinning occurring at lower shear rates. Both of these behaviors appear more frequently at fiber concentrations and aspect ratio relating to the *concentrated* régime. The source of the yield-like behavior is still inconclusive and needs to be further investigated. It is possibly a manifestation of one or both of the two most persuasive hypotheses. The first, being yield behavior is a result of dynamic fiber-fiber interaction. The second, yield behavior is due to long range networks formed by polymer-fiber entanglements.<sup>31, 79</sup> The discrepancies between glass fiber suspension that exhibit and do not exhibit a yield-like behavior could be a result of the variables in initial fiber orientation and how they are loaded into the rheometer and/or the degree of interaction with the suspending medium. The onset of shear thinning of a suspension at lower shear rates compared to the neat matrix is believed to be the result of an orientation distribution that is shear rate dependent.

The effect that glass fiber has on the elastic properties of Newtonian and non-Newtonian fluids is slightly ambiguous. The presence of normal stress differences in Newtonian suspensions and enhanced normal stress differences in non-Newtonian suspensions suggests that the presence of fiber enhances the elastic properties. However, if one takes the magnitude of the storage modulus as a measure of elasticity, then the absence of the storage modulus in Newtonian suspensions and the relatively unaffected storage modulus in non-Newtonian suspensions suggests that the presence of fiber has no

effect on the elasticity. Further evidence in support of this statement can be found in the relaxation spectrum of a suspension. Many authors have shown that the presence of fiber has little effect on the short relaxation times of a fluid. This is another indication that the elasticity is unaffected by the fiber. Also, the presence of fiber has been shown to decrease the extrudate swell. Work accomplished by Iso et al.<sup>47, 48</sup> and Sepehr et al.<sup>31</sup> has shown that the presence of fiber impedes the elasticity of viscoelastic fluids. The reviewed literature seems to suggest that the presence of the fiber acts to retard the elastic behavior of viscoelastic fluids and the enhanced normal stresses are a result of direct interaction between fibers.

Interrupted, unsteady shear flow experiments have led to the hypothesis that the evolution of the orientation distribution is specific to the kinematics of the flow and is irreversible.<sup>30</sup> A suspension whose initial fiber orientation is isotropic will exhibit a stress overshoot believed to be a result of the fibers rotating toward the flow direction. Ignoring the possible phenomena of quiescent orientation changes, the overshoot will only reappear if the sample is deformed in the opposite direction, and then at a delayed strain compared to the initial overshoot. Also, an initial normal stress difference overshoot typically occurs at a larger strain than the shear stress. Direct measurements of fiber orientation correlating to various rheological measurements would be invaluable in proving conclusive statements on fiber orientation effects on the unsteady shear flow rheology.

In extensional flow, the presence of fiber greatly enhances the steady-state tensile viscosity resulting in a Trouton ratio that can be an order of magnitude greater than the value three in the linear viscoelastic limit, and induces a large extension rate thinning behavior in non-Newtonian suspensions. The fiber also seems to suppress the strain thickening characteristics of the suspending medium. This is believed to be a result of induced shearing forces between fibers in extensional flow, dominating the kinematics.

### **Acknowledgment**

The financial support for this work from the National Science Foundation and Department of Energy through grant number DMI-0521918 is gratefully acknowledged.

1. Guo, R.; Azaiez, J.; Bellehumeur, C., Rheology of fiber filled polymer melts: Role of fiber-fiber interactions and polymer-fiber coupling. *Poly. Eng. Sci.* **2005**, 385-399.
2. Ganani, E.; Powell, R. L., Suspensions of rodlike particles: Literature review and data correlations. *J. Comp. Mat.* **1985**, 19, 194.
3. Zirnsak, M. A.; Hur, D. U.; Boger, D. V., Normal stresses in fibre suspensions. *J. Non-Newt. Fluid Mech.* **1994**, 54, 153-193.
4. Folkes, M. J., *Short Fibre Reinforced Thermoplastics*. Research Studies Press: New York, 1982.
5. Lefranche, E.; Drawczak, P.; Ciolczyk, J.-P.; Maugey, J., Injection moulding of long glass fiber reinforced polyamide 6,6: Processing conditions/microstructure/flexural properties relationship. *Adv. Poly. Technol.* **2005**, 24, (2), 114-131.
6. Cech, V.; Prikryl, R.; Balkova, R.; Grycova, A.; Vanek, J., Plasma surface treatment and modification of glass fibers. *Composites: Part A* **2002**, 33, 1367-1372.
7. Brown, E. N.; Davis, A. K.; Jonnalagadda, K. D.; Sottos, N. R., Effect of surface treatment on the hydrolytic stability of E-glass fiber bundle tensile strength. *Comp. Sci. Tech.* **2005**, 65, 129-136.
8. De, S. K.; White, J. R., *Short Fibre-Polymer Composites*. Woodhead Pub.: Cambridge, England, 1996.
9. Park, R.; Jang, J., Effect of surface treatment on the mechanical properties of glass fiber/vinylester composites. *J. Appl. Poly. Sci.* **2004**, 91, 3730-3736.
10. Lee, W.-G.; Hsu, T.-C. J.; Su, A. C., Interphase morphology of liquid crystalline polymer/glass fiber composites: Effect of surface treatment. *Macromolecules* **1994**, 27, 6551-6558.
11. Kalaprasad, G.; Thomas, S., Melt rheological behavior of intimately mixed short sisal-glass hybrid fiber-reinforced low-density polyethylene composites. II. Chemical Modification. *J. Applied Poly. Sci.* **2003**, 89, 443-450.
12. Li, R.; Ye, L.; Mai, Y.-W., Application of plasma technologies in reinforced polymer composites: A review of recent developments. *Composites: Part A* **1997**, 28, 73-86.
13. Doi, M.; Edwards, S. F., *The Theory of Polymer Dynamics*. Oxford University Press: New York, 1988.
14. Doi, M.; Kuzuu, N. Y., Non-linear elasticity of rodlike macromolecules in condensed state. *J. Poly. Sci. Part B - Poly Phys.* **1980**, 18, (3), 409-419.
15. Doi, M.; Edwards, S. F., Dynamics of rod-like macromolecules in concentrated solution. Part 1. *J. Chem. Soc. Faraday Trans.* **1977**, 74, (2), 560-570.
16. Batchelor, G. K., The stress generated in a non-dilute suspension of elongated particles by pure straining motion. *J. Fluid Mech.* **1971**, 46, 813-829.
17. Flory, P. J., Phase equilibria in solutions of rod-like particles. *Proc. R. Soc. London* **1956**, A234, 73-89.
18. Huq, A. M. A.; Azaiez, J., Effects of length distribution on the steady shear viscosity of semiconcentrated polymer-fiber suspensions. *Poly. Eng. Sci.* **2005**, 45, 1357-1368.
19. Kumar, K.; Bhatnagar, N.; Ghosh, A., Development of long glass fiber reinforced polypropylene composites: mechanical and morphological characteristics. *J. Reinf. Plastics Comp.* **2007**, 26, (3), 239-249.

20. Forgacs, O. L.; Mason, S. G., Particle motions in sheared suspensions IX. Spin and deformation of threadlike particles. *J. Colloid Sci.* **1958**, 14, 457-472.
21. Qi, D.; Cheng, G., Fatigue behavior of filament-wound glass fiber reinforced epoxy composite tubes under tension/torsion biaxial loading. *Poly. Comp.* **2007**, 28, (1), 116-123.
22. Ericsson, K. A.; Toll, S.; Manson, J.-A., Sliding plate rheometry of planar oriented concentrated fiber suspensions. *Rheol. Acta* **1997**, 36, 397-405.
23. Blankeney, W. R., Viscosity of suspensions of straight rigid rods. *J. Colloid Interface Sci.* **1966**, 22, (4), 324.
24. Milliken, W. J.; Mondy, L. A.; Gottlieb, M.; Graham, A. L.; Powell, R. L., The viscosity volume fraction relation for suspensions of randomly oriented rods by falling ball rheometry. *J. Non-Newt. Fluid Mech.* **1989**, 202, 217-232.
25. Nawab, M. A.; Mason, S. G., The viscosity of dilute suspensions of thread-like particles. *J. Physical Chem.* **1958**, 62, 1248-1253.
26. Powell, R. L., Rheology of suspensions of rodlike particles. *J. Stat. Phys.* **1990**, 62, 1073-1091.
27. Attanasio, A.; Bernini, U.; Galloppo, P.; Segre, G., Significance of viscosity measurements in macroscopic suspensions of elongated particles. *Trans. Soc. Rheol.* **1972**, 16, 147-154.
28. Mondy, L. A.; Geller, A. S.; Rader, D. J.; Ingber, M., Boundary element method calculations of the mobility of nonspherical particles. 2. Branched chains and flakes. *J. Aerosol Sci.* **1996**, 27, (4), 537-546.
29. Jeffery, G. B., The motion of ellipsoidal particles immersed in a viscous fluid. *Proc. R. Soc. Lond. A* **1922**, 102, 161-179.
30. Utracki, L. A., *Two-Phase Polymer Systems*. Oxford University Press: New York, 1991; p 277-331.
31. Sepehr, M.; Carreau, P. J.; Moan, M.; Ausias, G., Rheological properties of short fiber model suspensions. *J. Rheol.* **2004**, 48, (5), 1023-1048.
32. Owen, M. J., Flow, fiber orientation and mechanical property relationships in polyester DMC. *Proc. 33rd SPI Conf.* **1978**.
33. Laun, H. M., Orientation effects and rheology of short glass fiber-reinforced thermoplastics. *Colloid & Poly. Sci.* **1984**, 262, 257-269.
34. Segre, G.; Silberberg, A., Behaviour of macroscopic rigid spheres in Poiseuille flow. Part 1. Determination of local concentration by statistical analysis of particle passages through crossed light beams. *J. Fluid Mech.* **1962**, 14, 115-135.
35. Segre, G.; Silberberg, A., Behaviour of macroscopic rigid spheres in Poiseuille flow. Part 2. Experimental results and interpretation. *J. Fluid Mech.* **1962**, 14, 136-157.
36. Koh, C. J.; Hookham, P.; Leal, L. G., An experimental investigation of concentrated suspension flows in a rectangular channel. *J. Fluid Mech.* **1994**, 266, 1.
37. Wu, S., Order-disorder transitions in the extrusion of fiber-filled poly(ethylene terephthalate) and blends. *Poly. Eng. Sci.* **1979**, 19, 638-650.
38. Becraft, M. L.; Metzner, A. B., The rheology, fiber orientation, and processing behavior of fiber-filled fluids. *J. Rheol.* **1991**, 36, (1), 143-174.
39. Kalaprasad, G.; Mathew, G.; Pavithran, C.; Thomas, S., Melt rheological behavior of intimately mixed short sisal-glass hybrid fiber-reinforced low-density polyethylene composites. I. Untreated fibers. *J. Applied Poly. Sci.* **2003**, 89, 432-442.

40. Burgers, J. M., On the motion of small particles of elongated form suspended in a viscous liquid. Second report on viscosity and plasticity, chap. 3. *Kon. Ned. Akad. Wet. Verhand (Erste Sectie)* **1938**, 16, (4), 113-184.
41. Larson, R. G., *The Structure and Rheology of Complex Fluids*. Oxford University Press: New York, 1999.
42. Chaouche, M.; Koch, D. L., Rheology of non-Brownian rigid fiber suspensions with adhesive contacts. *J. Rheol.* **2001**, 45, (2), 369-382.
43. Dealy, J. M., Official nomenclature for material functions describing the response of a viscoelastic fluid to various shearing and extensional deformations. *J. Rheol.* **1995**, 39, (1), 253-265.
44. Ganani, E.; Powell, R. L., Rheological properties of rodlike particles in a Newtonian and a non-Newtonian fluid. *J. Rheol.* **1986**, 30, (5), 995-1013.
45. Han, C. D.; Lem, K. W., Rheology of unsaturated polyester resins. 1. Effects of filler and low-profile additive on the rheological behavior of unsaturated polyester resin. *J. Applied Poly. Sci.* **1983**, 28, (2), 743-762.
46. Mobuchon, C.; Carreau, P. J.; Heuzey, M.-C.; Sepehr, M.; Ausias, G., Shear and extensional properties of short glass fiber reinforced polypropylene. *Poly. Comp.* **2005**, 26, (3), 247-264.
47. Iso, Y.; Koch, D. L.; Cohen, C., Orientation in simple shear flow of semi-dilute fiber suspensions. 1. Weakly elastic fluids. *J. Non-Newt. Fluid Mech.* **1996**, 62, (2-3), 115-134.
48. Iso, Y.; Koch, D. L.; Cohen, C., Orientation in simple shear flow of semi-dilute fiber suspensions. 2. Highly elastic fluids. *J. Non-Newt. Fluid Mech.* **1996**, 62, (2-3), 135-153.
49. Mutel, A. T. Rheological behavior and fiber orientation in simple flow of glass fiber filled polypropylene melts. Ph. D., McGill University, 1989.
50. Macosko, C. W., *Rheology Principles, Measurements, and Applications*. Wiley-VCH: New York, 1994.
51. Baird, D. G.; Collias, D. I., *Polymer Processing*. John Wiley & Sons, Inc.: New York, 1998.
52. Greene, J. P.; Wilkes, J. O., Steady-state and dynamic properties of concentrated fiber-filled thermoplastics. *Poly. Eng. Sci.* **1995**, 35, (21), 1670-1681.
53. Carter, L. F. A study of the rheology of suspensions of rod-shaped particles in a Navier-Stokes liquid. Ph. D., University of Michigan, Ann Arbor, MI, 1967.
54. Faitel'son, L. A.; Kovtun, V. P., Experimental study of simple shear flow of monodisperse fibrous composites. *Polym. Mech.* **1975**, 11, 276-282.
55. Goto, S.; Nagazono, H.; Kato, H., The flow behavior of fiber suspensions in Newtonian fluids and polymer solutions. II: Capillary flow. *Rheol. Acta* **1986**, 25, 246-256.
56. Kitano, T.; Katoaka, T., The rheology of suspensions of vinylon fibers in polymer liquids. I. Suspensions in silicone oil. *Rheol. acta* **1981**, 20, 390-402.
57. Advani, S. G.; Tucker, C. L., The use of tensors to describe and predict fiber orientation in short fiber composites. *J. Rheol.* **1987**, 31, (8), 751-784.
58. Dinh, S. M.; Armstrong, R. C., A rheological equation of state for semiconcentrated fiber suspensions. *J. Rheol.* **1984**, 28, (3), 207-227.

59. Chan, Y.; White, J. L.; Oyanagi, Y., A fundamental study of the rheological properties of glass-fiber-reinforced polyethylene and polystyrene melts. *J. Rheol.* **1978**, 22, (5), 507-524.
60. Kim, J. K.; Song, J. H., Rheological properties and fiber orientation of short fiber-reinforced plastics. *J. Rheol.* **1997**, 41, (5), 1061-1085.
61. Thomasset, J.; Carreau, P. J., Rheological properties of long glass fiber filled polypropylene. *J. Non-Newt. Fluid Mech.* **2004**, 125, 25-34.
62. Mondy, L. A.; Morrison, T. G.; Graham, A. L.; Powell, R. L., Measurements of the viscosities of suspensions of oriented rods using falling ball rheometry. *Int. J. Multiphase Flow* **1990**, 16, (4), 651-662.
63. Cox, W. P.; Merz, E. H., Correlation of dynamic and steady flow viscosities. *J. Poly. Sci.* **1958**, 28, 619-622.
64. Bird, R. B.; Armstrong, R. C.; Hassager, O., *Dynamics of Polymeric Liquids*. John Wiley & Sons, Inc.: New York, 1987; Vol. 1.
65. Mutel, A. T.; Kamal, M. R., The effect of glass fibers on the rheological behavior of polypropylene melts between rotating parallel plates. *Poly. Comp.* **1984**, 5, (1), 29-35.
66. Drozdov, A. D.; Al-Mulla, A.; Gupta, R. K., The viscoelastic behavior of melts of virgin and recycled polycarbonate reinforced with short glass fibers. *Mechanics Research Communications* **2003**, 30, 595-614.
67. Kitano, T.; Kataoka, T.; Nagatsuka, Y., Dynamic flow properties of vinylon fiber and glass-fiber reinforced polyethylene melts. *Rheol. Acta* **1984**, 23, (4), 408-416.
68. Sepehr, M.; Ausias, G.; Carreau, P. J., Rheological properties of short fiber filled polypropylene in transient shear flow. *J. Non-Newt. Fluid Mech.* **2004**, 123, 19-32.
69. Ramazani, A.; Ait-Kadi, A.; Grmela, M., Rheology of fiber suspensions in viscoelastic media: Experiments and model predictions. *J. Rheol.* **2001**, 45, (4), 945-962.
70. Ivanov, Y.; VanDeVen, T. G. M.; Mason, S. G., Damped oscillations in the viscosity of suspensions of rigid rods. I. Monomodal suspensions. *J. Rheol.* **1982**, 26, (2), 213-230.
71. Okagawa, A.; Cox, R. G.; Mason, S. G., The kinetics of flowing dispersions. VI. Transient orientation and rheological phenomena of rods and discs in shear flow. *J. Colloid Interface Sci.* **1973**, 45, 303.
72. Ausias, G.; Agassant, J. F.; Vincent, M., Rheology of short glass fiber reinforced polypropylene. *J. Rheol.* **1992**, 36, (4), 525-542.
73. Mewis, J.; Metzner, A. B., The rheological properties of suspensions of fibers in Newtonian fluids subjected to extensional deformations. *J. Fluid Mech.* **1974**, 62, 593-600.
74. Weinberger, G. B.; Goddard, J. D., Extensional flow behavior of polymer solutions and particle suspensions in spinning motion. *Int. J. Multiphase Flow* **1974**, 1, 465-486.
75. Kamal, M. R.; Mutel, A. T.; Utracki, L. A., Elongational behavior of short glass fiber reinforced polypropylene melts. *Poly. Comp.* **1984**, 5, 289-298.
76. Creasy, T. S.; Advani, S. G., Transient rheological behavior of a long discontinuous fiber-melt system. *J. Rheol.* **1996**, 40, (4), 497-519.
77. Binding, D. M., An approximate analysis for contraction and converging flows. *J. Non-Newt. Fluid Mech.* **1988**, 27, 173-189.

78. Cogswell, F. N., Converging flow of polymer melts in extrusion dies. *Poly. Eng. Sci.* **1972**, 12, 64-73.
79. Zhang, W.; Komoto, S.; Takahashi, M.; White, J., Biaxial extensional flow behavior and fiber dispersion and orientation in short glass fiber filled polypropylene melts. *J. Soc. Rheol., Japan* **2001**, 29, (3), 111-120.
80. Creasy, T. S.; Advani, S. G., A model long-discontinuous-fiber filled thermoplastic melt in extensional flow. *J. Non-Newt. Fluid Mech.* **1997**, 73, 261-278.
81. Crowson, R. J.; Folkes, M. J.; Bright, P. F., Rheology of short glass fiber reinforced thermoplastics and its application to injection molding I. Fiber motions and viscosity measurements. *Poly. Eng. Sci.* **1980**, 20, 925-933.
82. Knuttson, B. A.; White, J. L., Rheological and extrusion characteristics of glass fiber reinforced polycarbonate. *J. Applied Poly. Sci.* **1981**, 26, 2347-2362.